Intrinsic properties of the two replicative DNA polymerases of Pyrococcus abyssi in replicating abasic sites: possible role in DNA damage tolerance?

Adeline Palud, Giuseppe Villani, Stéphane L'Haridon, Joël Querellou, Jean-Paul Raffin, Ghislaine Henneke

INTRINSIC PROPERTIES OF THE TWO REPLICATIVE DNA POLYMERASES OF PYROCOCCUS ABYSSI IN REPLICATING ABASIC SITES: POSSIBLE ROLE IN DNA DAMAGE TOLERANCE ?

Adeline Palud[1,2], Giuseppe Villani[3], Stéphane L'Haridon[2], Joël Querellou[1,2], Jean-Paul Raffin[1,2] and Ghislaine Henneke[1,2*]

1. Ifremer, UMR 6197, Laboratoire de Microbiologie des Environnements Extrêmes, BP 70, 29280 Plouzané, France.

2. Université de Bretagne Occidentale, UMR 6197, Laboratoire de Microbiologie des Environnements Extrêmes, 29280 Plouzané, France.

3. Institut de Pharmacologie et de Biologie Structurale, CNRS-Université Paul Sabatier Toulouse III, UMR 5089, 205 Route de Narbonne, 31077 Toulouse cedex, France.

Running Tittle : DNA synthesis by *Pab*pols of DNA containing abasic sites

*Corresponding author: Ghislaine HENNEKE, Ifremer, DEEP/LMEE, B.P. 70, 29280 Plouzané, France; Tel.: +33 2 98 22 46 09; Fax: +33 2 98 22 47 57

E-mail: ghenneke@ifremer.fr

Keywords: AP sites, Translesion, archaea, DNA polymerase

SUMMARY

Spontaneous and induced abasic sites in hyperthermophiles DNA have long been suspected to occur at high frequency. Here, *P.abyssi* was used as an attractive model to analyse the impact of such lesions onto the maintenance of genome integrity. We demonstrated that endogenous AP sites persist at a slightly higher level in *P.abyssi* genome compared to *E.coli*. Then, the two replicative DNA polymerases, *Pab*polB and *Pab*polD, were characterized in presence of DNA containing abasic sites. Both *Pab*pols had abortive DNA synthesis upon encountering AP sites. Under running start conditions, *Pab*polB could incorporate in front of the damage and even replicate to the full-length oligonucleotides containing a specific AP site , but only when present at a molar excess. Conversely, bypassing activity of *Pab*polD was strictly inhibited. The tight regulation of nucleotide incorporation opposite the AP site was assigned to the efficiency of the proofreading function, because exonuclease-deficient enzymes exhibited effective TLS. Steady-state kinetics reinforced that *Pab*pols are high-fidelity DNA polymerases onto undamaged DNA. Moreover, *Pab*pols preferentially inserted dAMP opposite an AP site, albeit inefficiently. While the template sequence of the oligonucleotides did not influence the nucleotide insertion, the DNA topology could impact on the progression of *Pab*pols. Our results are interpreted in terms of DNA damage tolerance.

INTRODUCTION

The genome of a living cell continuously undergoes a plethora of both exogenous or endogenous genotoxic attacks. Among the myriad of DNA lesions, the abasic [apurinic/apyrimidinic (AP)] sites are one of the most common lesions arising at high steady-state levels, yielding up to 2,000-10,000 lesions per human cell per day by spontaneous hydrolysis of the N-glycosylic bond (Lindahl and Nyberg, 1972; Lindahl, 1993). These lesions can be generated by direct elimination of bases via free radical attacks, as a consequence of cells exposure to chemical and physical agents (Breen and Murphy, 1995; Cadet *et al.*, 1999; Loeb *et al.*, 1986). Furthermore, AP sites appear transiently as intermediates of Base Excision Repair (BER) by DNA N-glycosylases (Loeb *et al.*, 1986; Scharer and Jiricny, 2001). Despite the fact that it could be considered as an attractive model, identification and determination of the mutagenic properties of AP sites in hyperthermophilic archaea (HA) remains poorly understood. Presumably, life at high temperature inflicts additional stress to genomic DNA in each cell and very high rates of potentially mutagenic DNA lesions (deamination, depurination, oxidation by hydrolytic mechanisms and subsequent strand breakage) should be expected. However, and interestingly, it was demonstrated that the hyperthermophilic crenarchaeon *Sulfolobus Acidocaldarius* exhibits a modest rate of spontaneous mutations nearly close to that of *Escherichia coli* (*E. coli)*, raising the question of how HA do to preserve their genome intact in such deleterious environmental conditions (Grogan *et al.*, 2001; Jacobs and Grogan, 1997).

To cope with the huge spectrum of impediments that result in genome destabilizing lesions, multiple DNA repair mechanisms have evolved in all organisms to ensure genomic stability (Friedberg *et al.*, 2006; Grogan, 2004; Hoeijmakers, 2001). However, situations can arise in which DNA damage escapes to DNA repair and persists into the genome. Cells have developed

DNA damage tolerance mechanisms to tolerate hurdles in DNA either by post-replicative gap filling, copy-choice DNA synthesis or translesion DNA synthesis (TLS) (Friedberg, 2005; Friedberg *et al.*, 2006). Both bacteria and eukaryotes can tolerate arrested DNA replication by template switching, therefore avoiding accumulation of mutations (Courcelle *et al.*, 2003; McGlynn and Lloyd, 2002). Whereas template switching systems remain unknown in archaea, TLS appears to be conserved within the three kingdoms of life (Boudsocq *et al.*, 2001; Friedberg *et al.*, 2000; Hubscher *et al.*, 2002; Nohmi, 2006; Pages and Fuchs, 2002; Shimizu *et al.*, 2003; Yang and Woodgate, 2007). Kinetically, this damage tolerance mechanism can be divided in two steps: (i) nucleotide insertion opposite the DNA lesion; (ii) extension beyond the lesion. Depending on the nature of the lesion, the bypass may involve a single or the concerted action of DNA polymerases (Friedberg, 2005; Friedberg *et al.*, 2005). High-fidelity replicative DNA polymerases in crenarchaea, bacteria and eukaryotes are intrinsically severely blocked upon incorporation opposite a lesion such as an abasic site, thus recognizing the illegitimate formed base pair and entering into futile cycles of insertion/excision (Gruz *et al.*, 2003; Pages *et al.*, 2005; Tanguy Le Gac *et al.*, 2004; Zhao *et al.*, 2004). This phenomenon called ‘idling’ is relevant to replicative DNA polymerases harbouring the proofreading 3’-5’ exonuclease and reflects the partitioning of a mispaired DNA template between the exonuclease/polymerase active sites (Villani *et al.*, 1978). The exonuclease activity acts as a kinetic barrier to TLS by preventing the stable incorporation of bases opposite the DNA lesion and, therefore, confers the exquisite accuracy of replicative DNA polymerases to preserve the integrity of the genome (Khare and Eckert, 2002). In the absence of coding information due to the base loss, most of replicative DNA polymerases obey to the A-rule, preferentially incorporating a dAMP opposite the abasic site (Haracska *et al.*, 2001; Lawrence *et al.*, 1990; Shibutani *et al.*, 1997).

Conceivably, the DNA sequence context, the structure of the DNA primer lesion and the replicative DNA polymerase examined can account for the preferential dAMP insertion opposite an abasic site. Currently, the A-rule for replicative DNA polymerases remains under intensive debates (Hogg *et al.*, 2004; Kroeger *et al.*, 2006; Taylor, 2002).

Here, we used *Pyrococcus abyssi* (*P. abyssi*), as a model for studying the genomic maintenance at high temperature. This euryarchaeote grows at an optimum of 95°C and is faced to environmental fluctuations imposed by hydrothermal vents (Erauso *et al.*, 1993; Jolivet *et al.*, 2003). Interestingly, *P. abyssi* is able to duplicate bidirectionally its 1.7 million base-pairs from a single origin as fast as 45 minutes (Myllykallio *et al.*, 2000) and DNA replication is thought to be achieved by the two high-fidelity DNA polymerases (*Pab*polD and *Pab*polB) and their accessory factors (Henneke *et al.*, 2005; Rouillon *et al.*, 2007). Consistent with the existing translesional systems and the lack of specialised DNA polymerases in *P. abyssi,* we speculate that one or both *Pab*pols could be involved in damage tolerance. In this study, we determine the steady-state level of AP sites in *E. coli* and *P. abyssi* at different growth stages. Secondly, we examine the bypass properties of the exonuclease proficient and deficient replicative *Pab*pols across an abasic site by varying the DNA topology and sequence context. Finally, steady-state kinetic was employed to give substantial insights into the role of the proofreading activity of *Pab*pols for nucleotide incorporation on damaged in comparison with intact DNA templates. Potential mutagenicity of abasic sites and more generally genomic maintenance in *P. abyssi* are discussed.

RESULTS

Rate of endogenous AP sites in *P. abyssi* and *E. coli*

Before dissecting the *in vitro* behaviour of the *Pab*pols in the presence of abasic sites, we investigated whether such DNA lesions were present into the genome of *P. abyssi.* The mesophilic bacteria *E. coli* was used as a control. The steady-state level of abasic sites was evaluated during the exponential and stationary phases of growth (Figure 1). In the exponential phase, 2 and 25 abasic sites per 100,000 bp were calculated for *E. coli* and *P. abyssi*, respectively (Figure 1). This value moderately increased to reach the number of 4 and 42 abasic sites per 100,000 bp at the stationary phase, for *E. coli* and *P. abyssi*, respectively. Taken together, these data provided evidence for the first time that the genome of the hyperthermophile *P. abyssi* has to deal with the presence of abasic sites. Further, the level of AP sites in *P. abyssi* genome is approximately 10-fold higher than in *E. coli*.

Replication of AP sites containing M13mp18 DNA template by *Pab*pols

We first checked the capacity of *Pab*pols to duplicate a circular AP-containing heteropolymeric M13mp18 DNA template. Preparation of this damaged AP-M13mp18 templates is depicted in Figure 2A. Under the conditions employed, 11 apurinic (the predominant lesion) and apyrimidinic sites are introduced per molecules (Schaaper and Loeb, 1981). *Pab*pols were tested in a primer extension assay in the presence of either abasic or undamaged M13mp18 templates. DNA elongation of the 5'-end fluorescein labelled oligonucleotide 6 (Table 1) was visualized by product analysis on alkaline agarose gel. In the presence of undamaged DNA template, both *Pab*pols (wild-type or exonuclease-deficient, respectively, exo+ and exo-) could extend the primer but with distinct efficiencies. While *Pab*polB exo+/exo- carried out DNA

synthesis to the full-length of the unmodified M13mp18 (7,249-nt), *Pab*polD exo+/exo- did only extend the primer to 3,600-nt likely due to its sensitivity to secondary structures as already observed (Henneke *et al.*, 2005) (Figure 2B, compare lanes 2 and 4 to 7 and 9). However, when *Pab*polD exo- elongated the undamaged template, a faint band corresponding to the full-length product was observed (Figure 2B, lane 9), consistent with the lower sensitivity of the *Pab*polD exo- to secondary structures. DNA synthesis reactions of the wild-type *Pab*pols with AP templates gave patterns similar to those obtained with undamaged templates, but with a lower amount of elongated products (Figure 2B, lanes 3 and 8). Therefore, the presence of abasic sites has an inhibitory effect on *Pab*pols activities. The results obtained with *Pab*pols were compared to those of T4 DNA polymerase, used as a control. While the relative distribution of the products of DNA replication was different with damaged versus undamaged M13mp18 DNA template, the lower efficiency of the T4 DNA polymerase (family B) in the presence of DNA lesions was confirmed (Figure 2B, lanes 12 and 13), as already described (Blanca *et al.*, 2007; Tanguy Le Gac *et al.*, 2004). It should be noted that, when reactions were carried out in the presence of *Pab*pols exo- with damaged DNA, a higher amount of replicated DNA products appeared (Figure 2B, compare lanes 3 to 5 for *Pab*polB and lanes 8 to 10 for *Pab*polD) indicating that the proofreading activity of *Pab*pols acts as a kinetic barrier to translesion synthesis onto damaged M13mp18. To further address the inhibitory effect of AP sites onto the DNA polymerising activity of *Pab*pols, quantitative analyses were performed by acid precipitable assay as described under Experimental procedures. Figure 2 C shows the results of replicating these DNA templates by *Pab*pols. Both *Pab*pols could discriminate between damaged and intact M13mp18 DNA template. Indeed, reduced synthetic rates were observed for *Pab*pols independently of the proficient or deficient exonuclease activity, with damaged DNA templates. The presence of AP

sites caused a more pronounced inhibition of replication by *Pab*polD, showing a 183-fold and 55-fold reduction of synthetic rates, respectively, for *Pab*polD exo+ and *Pab*polD exo-. In the case of *Pab*polB, a 6-fold and 5-fold reduction of synthetic rates, respectively, for *Pab*polB exo+ and *Pab*polB exo-, were caused by AP sites. T4 DNA polymerase (family B), used as a control, exhibited a reduced replicating activity comparable to that of *Pab*polB. Taken together, these results argued that *Pab*pols discriminate between undamaged or damaged DNA templates, with distinct reduced polymerising activities, suggesting that the presence of AP sites is rate-limiting.

Replication of AP-containing mini-circular and linear oligonucleotides DNA templates by the wild-type or exonuclease-deficient *Pab*polB

Since we provided evidence that DNA synthesis was severely impaired on damaged M13mp18 for both *Pab*pols, we further investigated the insights of such reduced activities. Translesional synthesis of a unique AP site from wild-type or exonuclease-deficient *Pab*pols were examined under running start conditions using either linear or mini-circular oligonucleotides DNA templates. The presence of the AP site was controlled by using T4 DNA polymerase as already described (Blanca *et al.*, 2007). While *Pab*polB exo+ could bypass the abasic site with moderate efficiency (63%) at a ratio enzyme / DNA of 4:1, under these conditions *Pab*polB exo- displayed almost full translesion synthesis (93%) (Figure 3A, compare lanes 7 and lanes 14, respectively for *Pab*polB exo+ and *Pab*polB exo-). Moreover, *Pab*polB exo+ had an increased capacity to stall at the AP site, as showed by the more marked presence of pausing sites at the lesion (Figure 3A, lanes 3-7). The efficiency of the bypass was dependent on the amount of the DNA polymerase used and the presence or absence of the 3'- to 5' exonuclease but, in all cases, a plateau could be reached near the equimolar enzyme / DNA

177 concentrations (Figure 3A, lanes 4-5 and lanes 11-12, respectively for *Pab*polB exo+ and
178 *Pab*polB exo-). The tolerance of the abasic site was reproducible and confirmed by using a linear
179 73-mer with a different DNA sequence context (data not shown) as already described (Tanguy
180 Le Gac *et al.*, 2004). When replicating the circular DNA template, the translesion ability of
181 *Pab*polB exo+/exo- was reduced at all enzyme concentrations tested. Interestingly, even at the
182 highest concentrations of *Pab*polB over the minicircle template, translesion synthesis across the
183 AP site for *Pab*polB exo+ only reached 32% at its peak (Figure 3B, lane 7) whereas it was much
184 more effective, reaching up to 86% for *Pab*polB exo- (Figure 3B, lane 13). In addition, under
185 these saturating conditions, there was a stimulation of strand displacement activity of the two
186 *Pab*polB versions, as indicated by the proportion of products longer than the 87-mer (Figure 3B,
187 lane 6-7 and 12-13). Taken together these results indicate that *Pab*polB has the capacity to
188 replicate past an AP site at high pol/DNA ratio. The proofreading activity of *Pab*polB influences
189 its translesion capacity and progression of both exonuclease-deficient and proficient *Pab*polB are
190 reduced in the presence of the mini-circular DNA template.
191
192 **Replication of AP-containing mini-circular and linear oligonucleotides DNA template by**
193 **the wild-type or exonuclease-deficient *Pab*polD**
194 The ability of *Pab*polD exo+/exo- to bypass an abasic site onto the linear and circular
195 oligonucleotides DNA templates was analysed and the results are presented in Figure 4. As it can
196 be seen, *Pab*polD exo+ could incorporate in front of the AP site but, contrary to *Pab*polB, could
197 not extend past the lesion both on linear and circular DNA templates at all the enzyme's
198 concentrations tested (lanes 3-7 in Figure 4A, and in Figure 4B). In addition, accumulation of a
199 shorter product at position +32 could be detected, indicating the 'idling' activity of the *Pab*polD

exo+. *Pab*polD exo- was also blocked at the AP site in the presence of the linear template but longer products past the AP site at position + 34, + 35, and + 36 could be detected, although they never reached the full-length of the 87-mer, even at saturating enzyme concentrations (Figure 4A, lanes 9-13). Interestingly, 35% of bypass could be measured at a ratio *Pab*polD exo - / DNA of 4:1 on the linear DNA template. Similarly, when the experiments were repeated in the presence of the minicircle DNA template, a strong block at the AP site (+ 33) could be observed for *Pab*polD exo - present at lower concentration to the DNA template (Figure 4B, lanes 9-10). Moreover, DNA synthesis continued past the AP site at position + 34, + 35, and + 36, but was also able to reach up to the full-length 87-mer (Figure 4B, lanes 11-13), when the concentration of the enzyme was higher than that of the minicircle DNA template. Therefore, in the case of *Pab*polD, its exonuclease activity prevents translesion synthesis of an abasic site independently of the structure of DNA template, while the exo – mutant shows some bypass capacity that seems enhanced in the case of a mini-circular DNA.

Steady-state kinetic analysis of nucleotide incorporation of wild-type and exonuclease-deficient *Pab*pols opposite undamaged bases

*Pab*pols have been designated as replicative DNA polymerases (Henneke *et al.*, 2005). This designation supposes that *Pab*pols must endow with high selectivity for each incoming nucleotide depending on the nature of the base-containing template. Nucleotide incorporation kinetics were measured in standing start reactions as described in Experimental procedures. Incorporation efficiency (k_{cat}/K_m) were measured for the wild-type and exonuclease-deficient *Pab*pols and the frequency of nucleotide misinsertion was calculated as the ratio of the efficiency (k_{cat}/K_m) of incorrect nucleotide incorporation to the efficiency (k_{cat}/K_m) of correct nucleotide

incorporation (Table 2). Both wild-type *Pab*pols exclusively incorporated the correct dGMP opposite template C and no misincorporation could be detected. In these conditions, a 5-fold reduced incorporation efficiency for *Pab*polD compared to *Pab*polB was observed as indicated by the k_{cat}/K_m values. The results obtained with the exonuclease-deficient *Pab*pols at template C showed that the correct dGMP was preferentially incorporated but their efficiencies were dramatically reduced compared to the wild-type enzymes, as judged from the dropped k_{cat}/K_m values, 55- and 103-fold, respectively, for *Pab*polB and *Pab*polD. In addition, misinsertion events by the exonuclease-deficient *Pab*pols at template C were comparable, with preference for insertion of dTMP > dAMP > dCMP (Table 2). Taken together, these results demonstrate that, while wild-type *Pab*pols monitor the instructional base of the template and discriminate between correct and incorrect nucleotides insertion, exonuclease-deficient *Pab*pols are much less efficient.

Steady-state kinetics analysis of nucleotide incorporation of wild-type and exonuclease-deficient *Pab*pols opposite an AP site

The efficiency for deoxynucleotide insertion opposite an abasic site for the wild-type *Pab*polB followed the order dAMP > dTMP and to a lesser extent dGMP. Interestingly, *Pab*polB exo + incorporated a dGMP 8355-fold less efficiently opposite an AP site than opposite the template C (Table 2). Similarly, as judged by the k_{cat}/K_m values, *Pab*polD exo + incorporated preferentially a dAMP over a dTMP opposite the abasic site with a 20-fold higher magnitude efficiency. It is noteworthy that the apparent K_m values from the incorporation of nucleotides opposite the abasic site were always higher than from the insertion of a correct dGMP at template C. Thus, proficient proofreading *Pab*pols are sensitive to abasic sites and are not

efficient at inserting a nucleotide opposite such a non-instructive lesion. As observed from the k_{cat}/K_m values, *Pab*pols exo - inserted a dAMP more efficiently than other deoxynucleotides opposite the AP site. While incorporation efficiencies of dAMP, dGMP and dTMP were higher when the proofreading function of *Pab*polB was deficient, no striking difference was observed between the wild-type and exonuclease-deficient *Pab*polD. Therefore, *Pab*polB and *Pab*polD exonuclease-deficient resemble each other in their ability to insert nucleotides opposite an abasic site with higher efficiencies for dAMP incorporation. Taken together, the data show that, while wild-type *Pab*polB does not significantly discriminate among nucleotides for incorporation opposite an AP site, the exonuclease-deficient *Pab*polB and both wild-type and exonuclease-deficient *Pab*polD were much sensitive to a non-coding lesion that seems to govern the dAMP incorporation rather than other dNTPs.

Effect of varying the downstream template base on nucleotide incorporation opposite an AP site by the *Pab*pols

The primer-templates used in these experiments were designed in order to examine the effect of changing the template base (N) at the 5' side of the AP site (X) on the initiation of the extension of the primer. Nucleotide incorporation was measured in standing start reactions under standard *Pab*pols assay conditions. The 32-mer primer (oligonucleotide 6) was annealed to the four templates differing by the nature of the base N = A, T, G and C at the 5' side of the AP site (Oligonucleotides 2, 1, 3, 4, respectively) (Figure 5). Extension of the primer in the four duplexes was conducted in the presence of each of the natural dNTPs. On the one hand, the wild-type *Pab*pols exclusively inserted a dAMP opposite the abasic lesion, independently of the sequence context (Figures 5A and 5B). While the percentages of incorporation of a dAMP

ranged from 46 to 58% for *Pab*polD exo+, they only reached 18% for *Pab*polB exo+. The *Pab*pols exo- also preferentially incorporated a dAMP opposite the AP site with a higher order of magnitude compared to the *Pab*pols exo+. For example, the percentages of incorporation of a dAMP ranged from 66 to 72% for *Pab*polD exo- and 46 to 58% for *Pab*polD exo+ (Figure 5D and Figure 5B, respectively). However, unlike *Pab*pols exo+, the *Pab*pols exo- also inserted other dNMPs opposite the non instructional lesion, following the order: dAMP>dGMP>dTMP>dCMP for *Pab*polB exo- and dAMP>dTMP~dCMP>dGMP for *Pab*polD exo-, independently of the sequence context (Figures 5C and 5D, respectively). Thus, these results demonstrate that nucleotide incorporation opposite an AP site by the *Pab*pols exo+/exo- is not directed by the nature of the base located at the 5' side of the AP site.

DISCUSSION

In hyperthermophiles, cellular and environmental stresses encountered by cells are likely to be exacerbated by adaptation to extreme conditions. Cell survival is ensured by a complex network of DNA events that contributes to the maintenance of the functional integrity of nucleic acids at high temperature. Here, we have focused the study on *P. abyssi*, an anaerobe hyperthermophilic euryarchaeota (HA) that thrives at elevated temperature in the immediate surroundings of deep-sea hydrothermal vents. This is the first report that establishes a relationship between the specific genomic level of abasic sites and the resulting impact on the intrinsic properties of replicative DNA polymerases in archaea. These features show that *P. abyssi* can be used as an informative model to analyse the biological relevance of DNA damage accumulation in the hyperthermophilic chromosome and the underlying genomic maintenance mechanisms.

The investigation presented here shows that the steady-state level of AP sites into the 1.7 million base-pairs of *P. abyssi* ranged from 25 to 42 AP sites per 100,000 bp during the exponential and stationary phases, respectively. Similarly, a 2-fold increase of AP sites is observed in *E. coli*. These findings corroborate the higher efficiency of DNA protection and repair mechanisms in proliferating cells, compatible with a low level of AP sites. However, it is important to precise that our expectation to detect a drastic increased number of abasic sites in the hyperthermophilic chromosome was not fulfilled. Indeed, the level was only 10-fold higher than in the mesophilic bacteria *E. coli*. Comparatively, the frequency of endogenous AP sites in mammalian cells reached 10 to 12 AP sites per 100,000 bp (Zhao *et al.*, 2006). Indeed, in the literature, the number of AP sites in the genome of thermophilic and hyperthermophilic microorganisms is always suspected to increase drastically compared to the mesophilic

counterparts (Grogan, 1998; Grogan, 2000). This assumption takes into account of the intrinsic properties of the primary structure of DNA at elevated temperatures, corresponding to a 3,000-fold increase in DNA decay at 100°C (Lindahl, 1993). Conceivably, *P. abyssi* has evolved to adjust genetically the level of endogenous AP sites in its genome that could be detrimental for genome integrity of mesophiles. Accumulation of AP sites and, more generally, others DNA lesions can be envisaged, suggesting that hyperthermophiles are adapted to survive pre-existing mutations. Clearly, these results establish that the number of AP sites seems to evolve respect to the growth stage without affecting cell growth and viability. However, further studies are required to determine the threshold that hyperthermophiles can support to ensure cell survival.

Evolution has produced multiple DNA polymerases able to replicate undamaged or damaged DNA. Sixteen DNA polymerases have been described in human, nine in *Saccharomyces cerevisiae*, five in *E. coli* (Bebenek and Kunkel, 2004; Hubscher *et al.*, 2002; Rothwell and Waksman, 2005) and up to five in archaea (Barry and Bell, 2006; Yang, 2005). Interestingly, the genome of the euryarchaeota *P. abyssi* encodes only two DNA polymerases, families B and D, required to faithfully duplicate the genetic information (Henneke *et al.*, 2005). In this study, steady-state kinetic analyses of nucleotide insertion show for the first time that *Pab*polD is endowed with high-fidelity onto undamaged DNA as its replicative counterpart, *Pab*polB (Table 2). Incorporation efficiency of *Pab*polD was reduced to five fold compared to *Pab*polB, demonstrating that *Pab*pols possesses distinct kinetic properties.

Our results give evidence that the presence of AP sites strongly inhibited the DNA polymerising activity of both *Pab*pols and that the absence of their proofreading function correlate with enhanced bypass of AP sites. The degree of inhibition of DNA synthesis was dependent upon the *Pab*pol examined. *Pab*polD could insert a nucleotide opposite the AP site and, in all conditions

tested, was not able to extend beyond the 3' primer lesion. *Pab*polB inserted opposite the AP site and extended the DNA template to the full-length, only when present at a molar excess over the template. This result is comparable to previous studies showing that molar excess of enzyme versus DNA template could enhance translesion synthesis by DNA polymerases past an abasic site (Blanca *et al.*, 2007; McCulloch and Kunkel, 2006; Tanguy Le Gac *et al.*, 2004). While translesion synthesis of both exonuclease-proficient and deficient *Pab*polBs and the exonuclease-deficient *Pab*polD were differently affected by the topology of the DNA template, the template sequence context did not significantly influence the bypass properties of *Pab*pols. Further, both *Pab*pols inserted dAMP opposite the AP site independently of the nature of the 5' template base to the AP site. Despite this nucleotide selectivity, steady-state kinetics showed that dAMP incorporation was not efficient. These observations show for the first time that archaeal replicative (families B and D) DNA polymerases follow the 'A-rule' (Strauss, 1991; Taylor, 2002) like eukaryal and bacterial counterparts (Haracska *et al.*, 2001; Shibutani *et al.*, 1997). The physical basis of the 'A-rule' is still an intensive debate (Kool, 2002; Zahn *et al.*, 2007) and structural studies reported the molecular level of replication blockage that produced catalytically inactive DNA polymerases (Freisinger *et al.*, 2004; Hogg *et al.*, 2004). Whether the molecular and physical bases are conserved through archaeal replicative DNA polymerases would have to be unravelled. Accordingly, the ability of abasic sites to inhibit *Pab*pols could reflect steric constraints imposed by the "tightness" of the active site. Furthermore, the capacity to partition the mispairs away from the polymerase domain into the exonuclease active site might exhibit structural rearrangements that are differentially influenced by the dynamic features of the DNA polymerase. To this point, the major distinction between the two *Pab*pols is the subunits composition. While *Pab*polB is a monomeric enzyme with associated exonuclease and

348 polymerase activities, *Pab*polD is an heterodimeric enzyme with the large and the small subunits
349 carrying, respectively, the polymerase and the exonuclease activities (Gueguen *et al.*, 2001).
350 Therefore, it is reasonable to suggest that the architecture of the two DNA polymerases may
351 account for the subtle differences observed within the polymerase and exonuclease efficiencies.
352 However, a complete detailed functional analysis must await the crystal structure of the
353 individual *Pab*pols. The balance between polymerization and excision was recently described in
354 B-family DNA polymerase in archaea (Kuroita *et al.*, 2005) but never in D-family. The distinct
355 kinetic partitioning of insertion and edition of mispairs observed within *Pab*pols corroborates
356 with eukaryal and bacterial homologues properties (Jin *et al.*, 2003; Jin *et al.*, 2005; Pages *et al.*,
357 2005) and confers that replicative DNA polymerases are high-fidelity enzymes (Bloom *et al.*,
358 1997; Chen *et al.*, 2000; Shimizu *et al.*, 2002).
359 The down-regulation of the proofreading function of *Pab*polB could favour TLS in order to
360 overcome the block imposed by AP sites. Bypass of AP sites could generate either single-base
361 substitutions or frameshift mutations (Baynton and Fuchs, 2000). *Pab*polB appears to proceed
362 through single-base substitution upon completion of DNA template containing an AP site. The
363 molar excess of the enzyme over the DNA template accounted for TLS under our *in vitro*
364 conditions. On the other hand, a replicative *Pab*pol idling at a DNA lesion could be a crucial
365 factor to trigger cellular responses to DNA damage in *P. abyssi*. The mechanism by which
366 proofreading activities of archaeal DNA polymerases could be regulated *in vivo* (dNTPs balance,
367 role of accessory proteins and enzymes switching) and their contribution in some cases to
368 counteract genomic DNA lesions has to be elucidated. Recently, it was described that *P. abyssi*
369 has evolved with efficient DNA strategies to cope with ionizing radiations and elevated
370 temperatures (Jolivet *et al.*, 2003). Biochemical evidence for relevant DNA repair mechanisms

has not been demonstrated in *P. abyssi* yet. More striking is the lack of identification of any mismatch repair genes and the complete set of damage excision genes (Cohen *et al.*, 2003). Interestingly, homologous recombination genes (RecA/Rad51) have been identified into the genome sequence of *P. abyssi* together with the fact that exponentially growing thermophilic archaea contain several copies of the chromosome (Bernander and Poplawski, 1997; Breuert *et al.*, 2006). This might be particularly consistent for the repair of strand breaks. Furthermore, it is not excluded that the recently characterised primase from *P. abyssi* could also play a role in damage avoidance since it possesses sequence and structural similarities with the family X DNA polymerases (Le Breton *et al.*, 2007). Ultimately, the process of such DNA lesions would have to be explored by the *P. abyssi* replisome in the context of genomic mutagenicity.

EXPERIMENTAL PROCEDURES

Strains and cell culture techniques

P. abyssi GE5 (Brittany Culture Collection, http://www.ifremer.fr/souchotheque) were grown in 50 ml YPS medium under anaerobic conditions at 95°C (Erauso *et al.*, 1993). The *E. coli* CIP 54.8 strain (CRBIP) was cultivated in 1 L of Luria-Bertani (LB) broth (1% tryptone, 0.5% yeast extract, 1% NaCl) at 37°C and pH 7.3, in a shaking incubator (170 rpm). Growth was monitored by density measurements with a cell Thoma counting chamber (0.02 mm depth). Samples for DNA extraction were collected in the exponential and stationary growth phases as indicated in Figure 1. The samples for DNA extraction were centrifuged at 6,000 g for 15 min at 4°C and the pellets were stored at –20°C.

Genomic DNA Isolation and Detection of AP sites

Genomic DNA from *P. abyssi* was isolated using the extraction method as described (Charbonnier *et al.*, 1995) and optimised in order to avoid the formation of additional AP sites. Briefly, cell pellets were suspended in 800 µl TE-Na-1 X lysis buffer (100 mM Tris-HCl, 50 mM EDTA, 100 mM NaCl, pH 8.0). This was followed by successive additions of 50 µl proteinase K (20 mg/ml), 100 µl Sarcosyl (10%), 100 µl SDS (10%). The applied lysis treatment were performed at 37°C for 1.5 hours and isolation of the total DNA was accomplished by adding an equal volume of buffered (pH 8.0) PCI (Phenol/Chloroform/Isoamyl Alcohol: 25/24/1). The samples were gently mixed and the aqueous phases were collected by centrifugation at 10,000 g for 10 min at 4°C. 10 µl RNAse (10 mg/ml) were added and incubation was performed at 37°C for one hour. DNAs were purified with an equal volume of PCI and centrifuged. The upper phase was extracted with an equal volume of pure chloroform and centrifuged. DNA precipitation was

obtained by mixing the final aqueous phase with 0.7 volume of 100% isopropanol followed by incubation for one hour at room temperature. After a 30 min centrifugation at 15,000 g at 4°C, the DNA pellets were washed once with 0.5 ml of 70% ice cold ethanol. Finally, the DNA pellets were air-dried during 1 hour before solubilization in TE-1X buffer (10 mM Tris-HCl, 2 mM EDTA, pH 7.5).

Genomic DNA extractions from *E. coli* was performed following the CTAB (Hexadecyl trimethyl-ammonium bromide) method for Gram-negative bacteria as described (Park, 2007).

The level of AP sites in genomic DNA was measured using the DNA damage quantification –AP site Counting kit from Dojindo Molecular Technologies (Gaithersburg, MD). DNA pellets were dissolved in TE buffer supplied by the kit and DNA concentrations were exactly adjusted to 100 ng/µl. Briefly, DNA samples were incubated with the Aldehyde Reactive Probe (ARP) reagent (N'-aminooxymethylcarbonylhydrazino-D-biotin) that specifically reacted with the aldehydic ring-opened AP sites (Kow and Dare, 2000; Kubo *et al.*, 1992). The AP sites tagged with biotin interacted with horseradish peroxidase-streptavidin and AP sites were colorimetrically detected. For each condition, the average of three measurements per sample was used in the statistical analyses.

Chemicals and Enzymes

Unlabelled dNTPs were from MP Biomedicals. T4 polynucleotide kinase, DNA ligase and T4 DNA polymerase were from New England Biolabs. *Pab*polD was cloned, expressed and purified as described (Henneke *et al.*, 2005). *Pab*polB (Isis DNA polymerase) and *Pab*polB exonuclease-deficient (Pyra DNA polymerase) were purchased from MP Biomedicals. 1 unit of *Pab*pols corresponds to the incorporation of 1 nmol of total dTMP into acid–precipitable

material per min at 65°C in a standard assay containing 0.5 μg (nucleotides) of poly(dA)/oligo(dT)$_{10:1}$. All other reagents were of analytical grade and purchased from Sigma-Aldrich and Fluka.

Construction, expression and purification of the recombinant wild-type and exonuclease-deficient His tag *Pab*polD

The pET26b expression vector containing the *Pab*polD large subunit (DP2) (Gueguen *et al.*, 2001) was digested with *Nde*I and *Sal*I and the resulting fragment was inserted into the pET28a expression vector (Novagen) in order to introduce a histidine tag (His tag) at the N-terminus. To render the *Pab*polD exonuclease-deficient, site-directed mutagenesis was carried out by introducing the H451A point mutation onto the *Pab*polD small subunit (DP1) (Gueguen *et al.*, 2001). The two site-specific complementary primers, reverse H451A 5'-TGGCCTAGCGGCATCGGCATTTCCTGGCCCTAT-3' and forward H451A 5'-ATAGGGCCAGGAAATGCCGATGCCGCTAGGCCA-3' were used to PCR amplify the pARHS expression vector containing DP1 according to the protocol of the Quick change Mutagenesis kit (Stratagene, La Jolla, CA). DNA sequencing was used to confirm that no spurious mutations had been introduced during PCR. The constructed expression vectors pET28a/DP2 and either the wild-type or the exonuclease-deficient pARHS/DP1 were co-introduced into host *E. coli* HMS174 (DE3). The transformed cells were grown in 1.5 liters Luria Bertani (LB) medium containing ampicillin (100 μg/ml) and kanamycin (30 μg/ml) at 37 °C. When A_{600} reached 0.7, 1 mM isopropylthio-β-D-galactoside was added to induce expression of active DNA polymerases. After being cultured 4 hours at 37 °C with gentle shaking (160 rpm), the cells were harvested by centrifugation, resuspended in 25 ml buffer A (20 mM sodium

450 phosphate, pH 6.6, 1 mM DTT, 20 mM Imidazole) containing the protease inhibitor, disrupted
451 on ice by French press and then heat-treated at 80°C for 15 min. Denatured host proteins were
452 removed by centrifugation. The clarified supernatant was applied further onto Ni^{2+}–HisTrap
453 column (5 ml of bed volume) pre-equilibrated with buffer A. Proteins were eluted with buffer B
454 (20 mM sodium phosphate, pH 6.6, 1 mM DTT, 500 mM Imidazole and active fractions were
455 pooled and dialysed against buffer C (20 mM sodium phosphate, pH 6.6, 1 mM DTT). The
456 dialysate was loaded onto a heparin column (5 ml of bed volume) pre-equilibrated with buffer D
457 (20 mM sodium phosphate, pH 6.6, 1 mM DTT, 0.15 M NaCl). The column was developed with
458 a linear gradient from buffer D to buffer E (20 mM sodium phosphate, pH 6.6, 1 mM DTT, 1 M
459 NaCl). Eluted protein showed over 98% purity. Pure His-*Pab*polD (wild-type and exonuclease-
460 deficient) were dialyzed against storage buffer (25 mM Tris–HCl, pH 8.0, 1 mM DTT, and 50%
461 glycerol) and stored at −20 °C until use. We checked by acid precipitable assay, as described
462 (Henneke *et al.*, 2005), that the addition of the His tag at the N terminus of DP2 had no effect on
463 the DNA polymerization activities. Moreover, the 3'-5' exonuclease deficiency for the mutant
464 H451A was confirmed (data not shown). Sequence alignment of exonuclease domain in
465 representative euryarchaeal DNA polymerases highlighting residues critical for proofreading
466 function is shown in Figure S1.
467
468 **Nucleic Acid Substrates**
469 Single-stranded (ss) M13mp18 was purchased (Amersham Biosciences, GE Healthcare).
470 In order to create AP sites into natural DNA templates, the ssM13mp18 viral DNA was
471 incubated at a final concentration of 0.18 pmol/µl in 30 mM potassium chloride, 10 mM sodium
472 citrate, pH 3.0 at 70°C for 45 min (Schaaper *et al.*, 1983). These conditions introduced one AP

473 sites per molecule in 4 min, measured by survival (Schaaper and Loeb, 1981). After treatment,
474 the damaged M13mp18 was purified with the QIAquick® PCR Purification Kit from Qiagen
475 (Germany).

476 The sequences of the DNA primers / templates used in the present study are depicted in
477 Table 1. All oligonucleotides, including those containing a tetrahydrofuran moiety mimicking an
478 abasic site, were chemically synthesized and gel-purified (Eurogentec, Belgium). Primers were
479 labelled at their 5'-end by fluorescein with the 5' End Tag kit labelling system from Vector
480 Laboratories (California). Free fluorescein was removed through the Microspin G-25 column
481 (Amersham Biosciences, GE Healtcare) and the labelled primers were hybridised to the
482 respective templates at equimolar concentrations.

483 The minicircle template was prepared as described (Tanguy Le Gac *et al.*, 2004). Briefly,
484 the linear 5'-phosphorylated oligonucleotide 1 (intact or containing the tetrahydrofuran moiety)
485 was intramolecularly ligated under dilute conditions using a scaffold 40-mer oligonucleotide (5'-
486 ATATTCCTACCCTCCCGATCTATCCACCATACTACCCTCC- 3'). Minicircles were gel-
487 purified and their concentration was determined spectrophotometrically, followed by annealing
488 with their complementary 5'-fluorescein labelled primer at equimolar concentration.

489

490 **Primer extension onto intact or damaged primed-oligonucleotides**

491 "Standing start" and "Running start" assays were catalysed into a final volume (15 µl)
492 containing the following components: (i) for *Pab*polD: 8.3 nM of labelled primers / templates, 20
493 nM of *Pab*polD exo+/exo- unless otherwise specified, 10 mM Tris-HCl (pH 9.0), 50 mM KCl,
494 10 mM $MgCl_2$ and 200 µM dNTPs; (ii) for *Pab*polB: 8.3 nM of labelled primers / templates, 13
495 nM of *Pab*polB exo+/exo- unless otherwise mentioned, 50 mM Tris-HCl (pH 8.8), 50 mM KCl,

1 mM DTT, 2 mM $MgCl_2$ and 200 µM dNTPs. Reactions were performed at 55°C for 30 minutes and quenched by the addition of 15 µl of stop buffer (98% formamide, 10 mM EDTA). Samples were heated at 95°C for 5 minutes. The reactions products were resolved on 15% polyacrylamide, 7 M urea gels and visualized with a Mode Imager Typhoon 9400 (Amersham Biosciences, GE Healthcare). Quantification of the results was performed using ImageQuant 5.2 software. The extent of the bypass reaction was calculated as the ratio of the intensity of the bands downstream of the AP site to the intensity of the bands opposite the lesion.

Effect of sequence context on AP site bypass was analysed under standing start conditions. The fluorescein-labelled primer (oligonucleotide 6) was annealed right before the template AP site that is indicated by X. Different template bases 5′ to the AP site are depicted by N (N=A, oligonucleotide 2; N=T, oligonucleotide 1; N=G, oligonucleotide 3; N=C, oligonucleotide 4) (Table 1). Bypass assays were performed as described above excepted that 16 nM of DNA templates were used when the template base 5' to the AP site was: N=T and N=C for *Pab*polB exo-, N=T and N=G for *Pab*polD exo+, N=C for *Pab*polB exo+. Quantification of nucleotides insertion opposite the AP site are calculated for wild-type and exonuclease-deficient *Pab*pols in triplicate but only the more resolving gel was quantified.

Steady-state Kinetic Analyses

A 5'-fluorescein labelled primer, annealed to either a correct or damaged template, was extended in the presence of increasing concentrations of a single dNTP. *Pab*pols concentrations and reaction times were set so that maximal product formation was ≤ 20% of the substrate concentration. The linear primer-template (oligonucleotides 6 and 1) was extended with dNTP at 55°C in the presence of 6.6-33.3 nM enzyme for 1 or 5 min, depending on the proper utilization

519 efficiency and substrate utilisation. All reactions (15 µl) were carried out at various dNTP
520 concentrations (in triplicate) and quenched with 2 volumes of a solution of 20 mM EDTA in 95%
521 formamide (v/v). Products were resolved using a 15% polyacrylamide (w/v) electrophoresis gel
522 containing 7 M urea and visualized using a Mode Imager Typhoon 9400. Bands were quantified
523 with ImageQuant 5.2 software (Amersham Biosciences, GE Healthcare). The observed rates of
524 deoxynucleotide incorporation as a function of dNTP concentration were firstly determined from
525 Lineweaver-Burk plots. The data were fit by nonlinear regression using the Marquardt-
526 Levenberg algorithm (EnzFitter 2.0, BioSoft) to the Michaelis-Menten equation describing a
527 hyperbola, v = (Vmax x [dNTP]/Km + [dNTP]) as already described (Le Breton *et al.*, 2007).
528 Apparent Km and Vmax kinetic parameters were obtained from the fit and were used to calculate
529 the efficiency of deoxynucleotide incorporation (k_{cat}/K_m). The kinetics values are the average of
530 at least triplicate determinations and are shown with standard deviations (SD). ND, means that
531 no detectable incorporation was observed. Gel patterns and quantitation of single nucleotide
532 incorporation reactions are shown in Figure S2.
533

534 **Primer extension onto intact or damaged M13mp18 DNA template**

535 *Product analysis*. The oligonucleotide 6 was annealed to either the damaged AP-
536 M13mp18 or undamaged M13mp18 at a molar ratio 3:1. Standard *Pab*pols reactions (10 µl) were
537 conducted into their respective buffer containing 200 µM each of dNTPs, 7 nM of DNA template
538 and 2 pmol of *Pab*pols. Reactions were carried out at 60°C for 30 minutes. T4 DNA polymerase
539 reactions were performed at 37°C for 30 minutes into the 1 X T4 pol buffer (according to the
540 manufacturer's protocol) with 7 nM of DNA template, 100 µM each of dNTPs and 2 pmol of T4
541 DNA polymerase. Reaction mixtures were stopped by the addition of 10 µl of 30 mM EDTA and

542 the samples were heated to 100°C for 10 min. Reactions mixtures were subjected to a 0.8% (w/v)
543 denaturing alkaline agarose gel electrophoresis, and replication products were visualized with a
544 Mode Imager Typhoon 9400 (Amersham Biosciences, GE Healthcare). DNA ladders (Raoul
545 markers, MP Biomedicals) were run into the same gel and revealed separately.

546 *Acid precipitable assay.* The reaction buffers composition were identical to those
547 described in product analysis for *Pab*pols and T4 DNA pol. The final volume of 10 µl contained
548 200 µM of unlabeled dNTPs, 20 µM [^{3}H]dTTP, 7 nM of DNA template (AP-M13mp18 or
549 undamaged M13mp18) and 2 pmol of enzyme to be tested. Reactions were carried out at 60°C
550 and 37°C, respectively, for *Pab*pols and T4 DNA pol for 30 minutes. DNA was precipitated with
551 10% trichloroacetic acid (TCA). Insoluble radioactive material was determined by scintillation
552 counting as described (Henneke *et al.*, 2005; Rouillon *et al.*, 2007).

ACKNOWLEDGEMENTS

We especially thank Kihei Kubo (Osaka Prefecture University, Sakai, Japan) for helpful technical comments on the Dojindo Kit. In addition, we thank Robert Fuchs for critical reading of the manuscript and very helpful discussions. This work was supported by IFREMER and the Région Bretagne. G.V. was supported by CNRS and ARC (grant 4969).

REFERENCES

Barry, E.R., and Bell, S.D. (2006) DNA replication in the archaea. *Microbiol Mol Biol Rev* **70**: 876-887.

Baynton, K., and Fuchs, R.P. (2000) Lesions in DNA: hurdles for polymerases. *Trends Biochem Sci* **25**: 74-79.

Bebenek, K., and Kunkel, T.A. (2004) Functions of DNA polymerases. *Adv Protein Chem* **69**: 137-165.

Bernander, R., and Poplawski, A. (1997) Cell cycle characteristics of thermophilic archaea. *J Bacteriol* **179**: 4963-4969.

Blanca, G., Delagoutte, E., Tanguy le Gac, N., Johnson, N.P., Baldacci, G., and Villani, G. (2007) Accessory proteins assist exonuclease-deficient bacteriophage T4 DNA polymerase in replicating past an abasic site. *Biochem J* **402**: 321-329.

Bloom, L.B., Chen, X., Fygenson, D.K., Turner, J., O'Donnell, M., and Goodman, M.F. (1997) Fidelity of Escherichia coli DNA polymerase III holoenzyme. The effects of beta, gamma complex processivity proteins and epsilon proofreading exonuclease on nucleotide misincorporation efficiencies. *J Biol Chem* **272**: 27919-27930.

Boudsocq, F., Iwai, S., Hanaoka, F., and Woodgate, R. (2001) Sulfolobus solfataricus P2 DNA polymerase IV (Dpo4): an archaeal DinB-like DNA polymerase with lesion-bypass properties akin to eukaryotic poleta. *Nucleic Acids Res* **29**: 4607-4616.

Breen, A.P., and Murphy, J.A. (1995) Reactions of oxyl radicals with DNA. *Free Radic Biol Med* **18**: 1033-1077.

Breuert, S., Allers, T., Spohn, G., and Soppa, J. (2006) Regulated polyploidy in halophilic archaea. *PLoS ONE* **1**: e92.

581 Cadet, J., Delatour, T., Douki, T., Gasparutto, D., Pouget, J.P., Ravanat, J.L., and Sauvaigo, S.
582 (1999) Hydroxyl radicals and DNA base damage. *Mutat Res* **424**: 9-21.
583 Charbonnier, F., Forterre, P., Erauso, G., and Prieur, D. (1995) Purification of Plasmids from
584 Thermophilic and Hyperthermophilic Archaea. In *Archaea: A Laboratory Manual*. F.T.
585 Robb, A.R.P. (ed): Cold Spring Harbor Laboratory Press, pp. 87-90.
586 Chen, X., Zuo, S., Kelman, Z., O'Donnell, M., Hurwitz, J., and Goodman, M.F. (2000) Fidelity
587 of eucaryotic DNA polymerase delta holoenzyme from Schizosaccharomyces pombe. *J*
588 *Biol Chem* **275**: 17677-17682.
589 Cohen, G.N., Barbe, V., Flament, D., Galperin, M., Heilig, R., Lecompte, O., Poch, O., Prieur,
590 D., Querellou, J., Ripp, R., Thierry, J.C., Van der Oost, J., Weissenbach, J., Zivanovic,
591 Y., and Forterre, P. (2003) An integrated analysis of the genome of the hyperthermophilic
592 archaeon Pyrococcus abyssi. *Mol Microbiol* **47**: 1495-1512.
593 Courcelle, J., Donaldson, J.R., Chow, K.H., and Courcelle, C.T. (2003) DNA damage-induced
594 replication fork regression and processing in Escherichia coli. *Science* **299**: 1064-1067.
595 Erauso, G., Reysenbach, A.L., Godfroy, A., Meunier, J.R., Crump, B., Partensky, F., Baross,
596 J.A., Marteinsson, V., Barbier, G., Pace, N.R., and Prieur, D. (1993) *Pyrococcus abyssi*
597 sp. nov., a new hyperthermophilic archaeon isolated from a deep-sea hydrothermal vent.
598 *Archives of Microbiology* **160**: 338-349.
599 Freisinger, E., Grollman, A.P., Miller, H., and Kisker, C. (2004) Lesion (in)tolerance reveals
600 insights into DNA replication fidelity. *Embo J* **23**: 1494-1505.
601 Friedberg, E.C., Feaver, W.J., and Gerlach, V.L. (2000) The many faces of DNA polymerases:
602 strategies for mutagenesis and for mutational avoidance. *Proc Natl Acad Sci U S A* **97**:
603 5681-5683.

604 Friedberg, E.C. (2005) Suffering in silence: the tolerance of DNA damage. *Nat Rev Mol Cell*
605 *Biol* **6**: 943-953.
606 Friedberg, E.C., Lehmann, A.R., and Fuchs, R.P. (2005) Trading places: how do DNA
607 polymerases switch during translesion DNA synthesis? *Mol Cell* **18**: 499-505.
608 Friedberg, E.C., Walker, G.C., Siede, W., Wood, R.D., Schultz, R.A., and Ellenberger, T. (2006)
609 Biological Responses to DNA Damage. In *DNA Repair and Mutagenesis*. Press, A. (ed).
610 Washington, D.C., pp. 3-7.
611 Grogan, D.W. (1998) Hyperthermophiles and the problem of DNA instability. *Molecular*
612 *Microbiology* **28**: 1043-1049.
613 Grogan, D.W. (2000) The question of DNA repair in hyperthermophilic archaea. *Trends*
614 *Microbiol* **8**: 180-185.
615 Grogan, D.W., Carver, G.T., and Drake, J.W. (2001) Genetic fidelity under harsh conditions:
616 analysis of spontaneous mutation in the thermoacidophilic archaeon Sulfolobus
617 acidocaldarius. *Proc Natl Acad Sci U S A* **98**: 7928-7933.
618 Grogan, D.W. (2004) Stability and repair of DNA in hyperthermophilic Archaea. *Curr Issues*
619 *Mol Biol* **6**: 137-144.
620 Gruz, P., Shimizu, M., Pisani, F.M., De Felice, M., Kanke, Y., and Nohmi, T. (2003) Processing
621 of DNA lesions by archaeal DNA polymerases from Sulfolobus solfataricus. *Nucleic*
622 *Acids Res* **31**: 4024-4030.
623 Gueguen, Y., Rolland, J.L., Lecompte, O., Azam, P., Le Romancer, G., Flament, D., Raffin, J.P.,
624 and Dietrich, J. (2001) Characterization of two DNA polymerases from the
625 hyperthermophilic euryarchaeon Pyrococcus abyssi. *Eur J Biochem* **268**: 5961-5969.

626 Haracska, L., Unk, I., Johnson, R.E., Johansson, E., Burgers, P.M., Prakash, S., and Prakash, L.
627 (2001) Roles of yeast DNA polymerases delta and zeta and of Rev1 in the bypass of
628 abasic sites. *Genes Dev* **15**: 945-954.
629 Henneke, G., Flament, D., Hubscher, U., Querellou, J., and Raffin, J.P. (2005) The
630 hyperthermophilic euryarchaeota Pyrococcus abyssi likely requires the two DNA
631 polymerases D and B for DNA replication. *J Mol Biol* **350**: 53-64.
632 Hoeijmakers, J.H. (2001) Genome maintenance mechanisms for preventing cancer. *Nature* **411**:
633 366-374.
634 Hogg, M., Wallace, S.S., and Doublie, S. (2004) Crystallographic snapshots of a replicative
635 DNA polymerase encountering an abasic site. *Embo J* **23**: 1483-1493.
636 Hubscher, U., Maga, G., and Spadari, S. (2002) Eukaryotic DNA polymerases. *Annu Rev*
637 *Biochem* **71**: 133-163.
638 Jacobs, K.L., and Grogan, D.W. (1997) Rates of spontaneous mutation in an archaeon from
639 geothermal environments. *J Bacteriol* **179**: 3298-3303.
640 Jin, Y.H., Ayyagari, R., Resnick, M.A., Gordenin, D.A., and Burgers, P.M. (2003) Okazaki
641 fragment maturation in yeast. II. Cooperation between the polymerase and 3'-5'-
642 exonuclease activities of Pol delta in the creation of a ligatable nick. *J Biol Chem* **278**:
643 1626-1633.
644 Jin, Y.H., Garg, P., Stith, C.M., Al-Refai, H., Sterling, J.F., Murray, L.J., Kunkel, T.A., Resnick,
645 M.A., Burgers, P.M., and Gordenin, D.A. (2005) The multiple biological roles of the 3'--
646 >5' exonuclease of Saccharomyces cerevisiae DNA polymerase delta require switching
647 between the polymerase and exonuclease domains. *Mol Cell Biol* **25**: 461-471.

Jolivet, E., Matsunaga, F., Ishino, Y., Forterre, P., Prieur, D., and Myllykallio, H. (2003) Physiological responses of the hyperthermophilic archaeon "Pyrococcus abyssi" to DNA damage caused by ionizing radiation. *J Bacteriol* **185**: 3958-3961.

Khare, V., and Eckert, K.A. (2002) The proofreading 3'-->5' exonuclease activity of DNA polymerases: a kinetic barrier to translesion DNA synthesis. *Mutat Res* **510**: 45-54.

Kool, E.T. (2002) Active site tightness and substrate fit in DNA replication. *Annu Rev Biochem* **71**: 191-219.

Kow, Y.W., and Dare, A. (2000) Detection of abasic sites and oxidative DNA base damage using an ELISA-like assay. *Methods* **22**: 164-169.

Kroeger, K.M., Kim, J., Goodman, M.F., and Greenberg, M.M. (2006) Replication of an oxidized abasic site in Escherichia coli by a dNTP-stabilized misalignment mechanism that reads upstream and downstream nucleotides. *Biochemistry* **45**: 5048-5056.

Kubo, K., Ide, H., Wallace, S.S., and Kow, Y.W. (1992) A novel, sensitive, and specific assay for abasic sites, the most commonly produced DNA lesion. *Biochemistry* **31**: 3703-3708.

Kuroita, T., Matsumura, H., Yokota, N., Kitabayashi, M., Hashimoto, H., Inoue, T., Imanaka, T., and Kai, Y. (2005) Structural mechanism for coordination of proofreading and polymerase activities in archaeal DNA polymerases. *J Mol Biol* **351**: 291-298.

Lawrence, C.W., Borden, A., Banerjee, S.K., and LeClerc, J.E. (1990) Mutation frequency and spectrum resulting from a single abasic site in a single-stranded vector. *Nucleic Acids Res* **18**: 2153-2157.

Le Breton, M., Henneke, G., Norais, C., Flament, D., Myllykallio, H., Querellou, J., and Raffin, J.P. (2007) The heterodimeric primase from the euryarchaeon Pyrococcus abyssi: a multifunctional enzyme for initiation and repair? *J Mol Biol* **374**: 1172-1185.

671 Lindahl, T., and Nyberg, B. (1972) Rate of depurination of native deoxyribonucleic acid.
672 *Biochemistry* **11**: 3610-3618.
673 Lindahl, T. (1993) Instability and decay of the primary structure of DNA. *Nature* **362**: 709-715.
674 Loeb, L.A., Preston, B.D., Snow, E.T., and Schaaper, R.M. (1986) Apurinic sites as common
675 intermediates in mutagenesis. *Basic Life Sci* **38**: 341-347.
676 McCulloch, S.D., and Kunkel, T.A. (2006) Multiple solutions to inefficient lesion bypass by T7
677 DNA polymerase. *DNA Repair (Amst)* **5**: 1373-1383.
678 McGlynn, P., and Lloyd, R.G. (2002) Recombinational repair and restart of damaged replication
679 forks. *Nat Rev Mol Cell Biol* **3**: 859-870.
680 Myllykallio, H., Lopez, P., Lopez Garcia, P., Heilig, R., Saurin, W., Zivanovic, Y., Philippe, H.,
681 and Forterre, P. (2000) Bacterial mode of replication with eukaryotic-like machinery in a
682 hyperthermophilic archaeon. *Science* **288**: 2212-2215.
683 Nohmi, T. (2006) Environmental Stress and Lesion-Bypass DNA Polymerases. *Annu Rev*
684 *Microbiol*.
685 Pages, V., and Fuchs, R.P. (2002) How DNA lesions are turned into mutations within cells?
686 *Oncogene* **21**: 8957-8966.
687 Pages, V., Janel-Bintz, R., and Fuchs, R.P. (2005) Pol III proofreading activity prevents lesion
688 bypass as evidenced by its molecular signature within E.coli cells. *J Mol Biol* **352**: 501-
689 509.
690 Park, D. (2007) Genomic DNA isolation from different biological materials. *Methods Mol Biol*
691 **353**: 3-13.
692 Rothwell, P.J., and Waksman, G. (2005) Structure and mechanism of DNA polymerases. *Adv*
693 *Protein Chem* **71**: 401-440.

694 Rouillon, C., Henneke, G., Flament, D., Querellou, J., and Raffin, J.P. (2007) DNA Polymerase
695 Switching on Homotrimeric PCNA at the Replication Fork of the Euryarchaea
696 Pyrococcus abyssi. *J Mol Biol* **369**: 343-355.
697 Schaaper, R.M., and Loeb, L.A. (1981) Depurination causes mutations in SOS-induced cells.
698 *Proc Natl Acad Sci U S A* **78**: 1773-1777.
699 Schaaper, R.M., Kunkel, T.A., and Loeb, L.A. (1983) Infidelity of DNA synthesis associated
700 with bypass of apurinic sites. *Proc Natl Acad Sci U S A* **80**: 487-491.
701 Scharer, O.D., and Jiricny, J. (2001) Recent progress in the biology, chemistry and structural
702 biology of DNA glycosylases. *Bioessays* **23**: 270-281.
703 Shibutani, S., Takeshita, M., and Grollman, A.P. (1997) Translesional synthesis on DNA
704 templates containing a single abasic site. A mechanistic study of the "A rule". *J Biol*
705 *Chem* **272**: 13916-13922.
706 Shimizu, K., Hashimoto, K., Kirchner, J.M., Nakai, W., Nishikawa, H., Resnick, M.A., and
707 Sugino, A. (2002) Fidelity of DNA polymerase epsilon holoenzyme from budding yeast
708 Saccharomyces cerevisiae. *J Biol Chem* **277**: 37422-37429.
709 Shimizu, M., Gruz, P., Kamiya, H., Kim, S.R., Pisani, F.M., Masutani, C., Kanke, Y.,
710 Harashima, H., Hanaoka, F., and Nohmi, T. (2003) Erroneous incorporation of oxidized
711 DNA precursors by Y-family DNA polymerases. *EMBO Rep* **4**: 269-273.
712 Strauss, B.S. (1991) The 'A rule' of mutagen specificity: a consequence of DNA polymerase
713 bypass of non-instructional lesions? *Bioessays* **13**: 79-84.
714 Tanguy Le Gac, N., Delagoutte, E., Germain, M., and Villani, G. (2004) Inactivation of the 3'-5'
715 exonuclease of the replicative T4 DNA polymerase allows translesion DNA synthesis at
716 an abasic site. *J Mol Biol* **336**: 1023-1034.

717 Taylor, J.S. (2002) New structural and mechanistic insight into the A-rule and the instructional
718 and non-instructional behavior of DNA photoproducts and other lesions. *Mutat Res* **510**:
719 55-70.
720 Villani, G., Boiteux, S., and Radman, M. (1978) Mechanism of ultraviolet-induced mutagenesis:
721 extent and fidelity of in vitro DNA synthesis on irradiated templates. *Proc Natl Acad Sci*
722 *U S A* **75**: 3037-3041.
723 Yang, W. (2005) Portraits of a Y-family DNA polymerase. *FEBS Lett* **579**: 868-872.
724 Yang, W., and Woodgate, R. (2007) What a difference a decade makes: insights into translesion
725 DNA synthesis. *Proc Natl Acad Sci U S A* **104**: 15591-15598.
726 Zahn, K.E., Belrhali, H., Wallace, S.S., and Doublie, S. (2007) Caught bending the A-rule:
727 crystal structures of translesion DNA synthesis with a non-natural nucleotide.
728 *Biochemistry* **46**: 10551-10561.
729 Zhao, B., Xie, Z., Shen, H., and Wang, Z. (2004) Role of DNA polymerase eta in the bypass of
730 abasic sites in yeast cells. *Nucleic Acids Res* **32**: 3984-3994.
731 Zhao, H., Shen, J., Deininger, P., and Hunt, J.D. (2006) Abasic sites and survival in resected
732 patients with non-small cell lung cancer. *Cancer Lett*.
733
734

735 **FIGURE LEGENDS**

736 **Table 1. Damaged or intact oligonucleotides used in this study.** X represents the position of
737 the correct base, template C, or a tetrahydrofuran moiety designed to functionally mimic an
738 abasic site.

739

740 **Table 2**. **Incorporation kinetics by wild-type and exonuclease-deficient *Pab*pols.** Single
741 nucleotide insertion assays were performed as described in Experimental procedures. The
742 observed rates of deoxynucleotide incorporation as a function of dNTP concentration were firstly
743 determined from Lineweaver-Burk plots. The data were fit by nonlinear regression using the
744 Marquardt-Levenberg algorithm (EnzFitter 2.0, BioSoft) to the Michaelis-Menten equation
745 describing a hyperbola, v = (Vmax x [dNTP]/Km + [dNTP]) as already described (Le Breton *et*
746 *al.*, 2007). Apparent Km and Vmax kinetic parameters were obtained from the fit and were used
747 to calculate the efficiency of deoxynucleotide incorporation (k_{cat}/K_m). The kinetics values are the
748 average of at least triplicate determinations and are shown with SD. The *f*(misinsertion
749 frequency) is the ratio k_{cat}/K_m for the incorrect nucleotide to k_{cat}/K_m for the correct nucleotide. ND
750 means no detectable incorporation observed.

751

752 **Figure 1. Rate of endogenous AP sites into *P. abyssi* and *E.coli* genomes at different growth**
753 **stages.** Steady-state level of AP sites per 100,000 bp was calculated during the exponential and
754 stationary phases of growth. The number of AP sites per 100,000 bp represents the mean of
755 triplicate experiments and error bars show the standard deviations of each measurement.

756

Figure 2. Replication of AP sites containing M13mp18 DNA template by *Pab*pols. A, Chemical treatment to induced AP sites into M13mp18 DNA. **B,** Primer extension assays were performed with 5'-fluorescein end labelled primer (oligonucleotide 6) hybridised to either the damaged or undamaged M13mp18 DNA template, *Pab*pols and T4 DNA polymerase used as a control experiment. The elongated products were separated on a 0.8 % (w/v) denaturing alkaline agarose gel. Lanes 1, 2, 4, 6, 7, 9, 11, 12 are the undamaged extended products; lanes 3, 5, 8, 10, 13 are the damaged extended products. **C**, dNTPs incorporation into the damaged and undamaged M13mp18 DNA primed-templates were tested by acid precipitation and incubation was performed according to the dependent polymerase reactions with [^{3}H]dTTP as the substrate (as outlined in Experimental procedures).

Figure 3. Replication of AP-containing mini-circular and linear oligonucleotides DNA templates by the wild-type or exonuclease-deficient *Pab*polB. Primer extension assays were performed at the indicated *Pab*polB concentrations with 8.3 nM of primer-template (oligonucleotides 1 and 5), 200 μM dNTPs at 55°C for 30 min as described in the Experimental procedures. Quantifications of the extended products from the AP site are mentioned below the gels. The extent of the bypass reaction was calculated as the ratio of the intensity of the bands downstream of the AP site to the intensity of the bands opposite the lesion. **A,** Replication onto the AP site-containing linear template. The position of the abasic site is indicated by X. Lanes 2 and 9 correspond to the positive control with 8.3 nM of intact template (X=C). **B,** Replication of the AP site-containing circular template. Lanes 2 and 8 correspond to the positive control with 8.3 nM of intact template (X=C). 32 mer indicates the position of the base preceding the AP site, while 33 mer is the position of the AP site.

Figure 4. Replication of AP-containing mini-circular and linear oligonucleotides DNA templates by the wild-type or exonuclease-deficient *Pab*polD. Primer extension assays were performed at the indicated *Pab*polD concentrations with 8.3 nM of primer-template (oligonucleotides 1 and 5), 200 μM dNTPs at 55°C for 30 min as described in the Experimental procedures. Quantification of the extended products from the AP site is mentioned below the gels. The extent of the bypass reaction was calculated as the ratio of the intensity of the bands downstream of the AP site to the intensity of the bands opposite the lesion. **A,** Replication onto the AP site-containing linear template. The position of the abasic site is indicated by X. Lanes 2 and 8 correspond to the positive control with 8.3 nM of template (X=C). **B,** Replication of the AP site-containing circular template. Lanes 2 and 8 correspond to the positive control with 8.3

nM of template (X=C). 32 mer indicates the position of the base preceding the AP site, while 33 mer is the position of the AP site.

Figure 5. Effect of varying the downstream template base on nucleotide incorporation opposite an AP site by *Pab*pols. Standing start reactions were performed with four DNA templates that varied by the nature of the 5' template base. The fluorescein-labelled primer (oligonucleotide 6) was annealed right before the template AP site that is indicated by X. Different template bases 5′ to the AP site are depicted by N (N=A, oligonucleotide 2; N=T, oligonucleotide 1; N=G, oligonucleotide 3; N=C, oligonucleotide 4) (Table 1). Single nucleotide incorporations were carried out as described in Experimental procedures with the different primed-templates, 13 nM of *Pab*polB exo+/exo-, 20 nM of *Pab*polD exo+/exo-, 200 μM of each dNTP at 55°C for 30 min. A. Reaction with 13 nM *Pab*polB exo+. B. Reaction with 20 nM *Pab*polD exo+. C. Reaction with 13 nM *Pab*polB exo-. D. Reaction with 20 nM *Pab*polD exo+.

804

Oligonucleotide 1
5'-CAGGAAACAGCTATGACCATGATTACGAATTCGAGCTCGGTACCCGGGGATCC**TX**TAGAGTCGACCTGCAGGCATGCAAGCTTGGCA-3'
Oligonucleotide 2
5'-CAGGAAACAGCTATGACCATGATTACGAATTCGAGCTCGGTACCCGGGGATCC**AX**TAGAGTCGACCTGCAGGCATGCAAGCTTGGCA-3'
Oligonucleotide 3
5'-CAGGAAACAGCTATGACCATGATTACGAATTCGAGCTCGGTACCCGGGGATCC**GX**TAGAGTCGACCTGCAGGCATGCAAGCTTGGCA-3'
Oligonucleotide 4
5'-CAGGAAACAGCTATGACCATGATTACGAATTCGAGCTCGGTACCCGGGGATCC**CX**TAGAGTCGACCTGCAGGCATGCAAGCTTGGCA-3'
Oligonucleotide 5
5′-TGCCAAGCTTGCATGCC-3′
Oligonucleotide 6
5′-TGCCAAGCTTGCATGCCTGCAGGTCGACTCTA-3′

805

806 **Table 1 : Damaged or intact oligonucleotides used in this study**

807

	DNA polymerase	dNTP	*Km* (μM)	*kcat* (min^{-1})	*kcat/Km* (μM^{-1} min^{-1})	*f*(misinsertion frequency)
Insertion opposite C	*Pab*polB exo+	dATP	ND	ND	ND	
		dTTP	ND	ND	ND	
		dGTP	0.25±0.01	425.27 ±0.12	1671.5	
		dCTP	ND	ND	ND	
	*Pab*polD exo+	dATP	ND	ND	ND	
		dTTP	ND	ND	ND	
		dGTP	0.19±0.02	66.70±0.69	346.36	
		dCTP	ND	ND	ND	
	*Pab*polB exo-	dATP	18.70±1.23	61.09±0.43	3.27	0.11
		dTTP	5.46±0.05	35.05±0.86	6.42	0.21
		dGTP	1.98±0.35	60.29±0.15	30.41	1.00
		dCTP	32.01±2.11	23.07±0.37	0.72	0.02
	*Pab*polD exo-	dATP	74.47±9.16	39.71±1.28	0.53	0.16
		dTTP	17.00±3.50	32.50±1.30	1.91	0.57
		dGTP	13.93±1.08	46.81±8.60	3.36	1.00
		dCTP	374.69±129.32	10.41±8.20	0.03	0.01
Insertion opposite AP site	*Pab*polB exo+	dATP	100±9	87±4	0.79	
		dTTP	121±7	91±4	0.75	
		dGTP	610±40	120±8	0.20	
		dCTP	ND	ND	ND	
	*Pab*polD exo+	dATP	36±3	114±4	3.17	
		dTTP	650±20	102±2	0.16	
		dGTP	ND	ND	ND	
		dCTP	ND	ND	ND	
	*Pab*polB exo-	dATP	4.19±0. 31	89.42±1.23	21.35	
		dTTP	15.02±0. 18	62.92±0. 11	4.19	
		dGTP	8.88± 2.35	73.68±4.71	8.30	
		dCTP	ND	ND	ND	
	*Pab*polD exo-	dATP	12.00±2.41	29.03±1.32	2.42	
		dTTP	76.19±0. 85	25.55±0. 07	0.34	
		dGTP	70.41±7.61	12.43±0. 36	0.18	
		dCTP	82.08±6.12	30.72±0. 54	0.37	

808
809
810 **Table 2 : Incorporation kinetics by wild-type and exonuclease-deficient *Pab*pols**
811
812

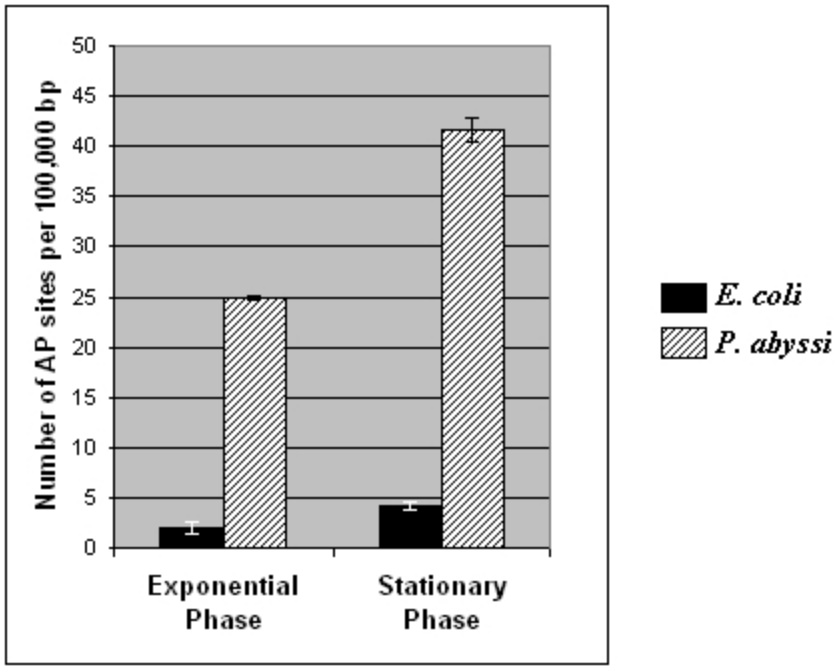
Number of AP sites per 100,000 bp
50
45
40
35
30
25
20
15
10
5
0
Exponential Phase
Stationary Phase
E. coli
P. abyssi

Figure1

Figure 2

A.

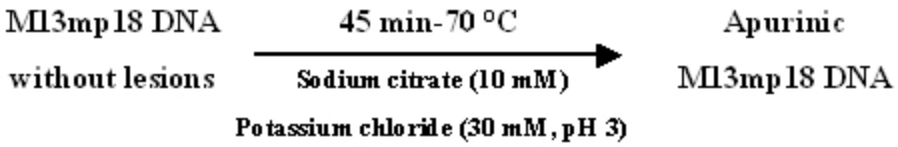
M13mp18 DNA
without lesions
45 min-70 °C
Sodium citrate (10 mM)
Potassium chloride (30 mM, pH 3)
Apurinic
M13mp18 DNA

B.

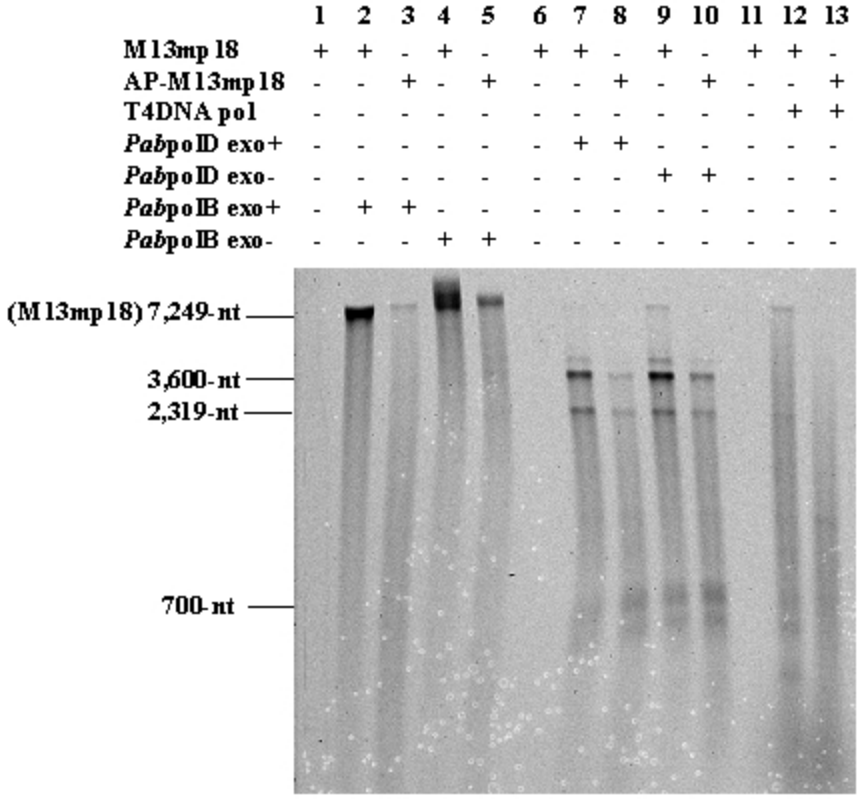
1 2 3 4 5 6 7 8 9 10 11 12 13
M13mp18 + + - + - + + - + - + + -
AP-M13mp18 - - + - + - - + - + - - +
T4DNA pol - - - - - - - - - - - + +
PabpoID exo+ - - - - - - + + - - - - -
PabpoID exo- - - - - - - - - + + - - -
PabpoIB exo+ - + + - - - - - - - - - -
PabpoIB exo- - - - + + - - - - - - - -
(M13mp18) 7,249-nt
3,600-nt
2,319-nt
700-nt

C.

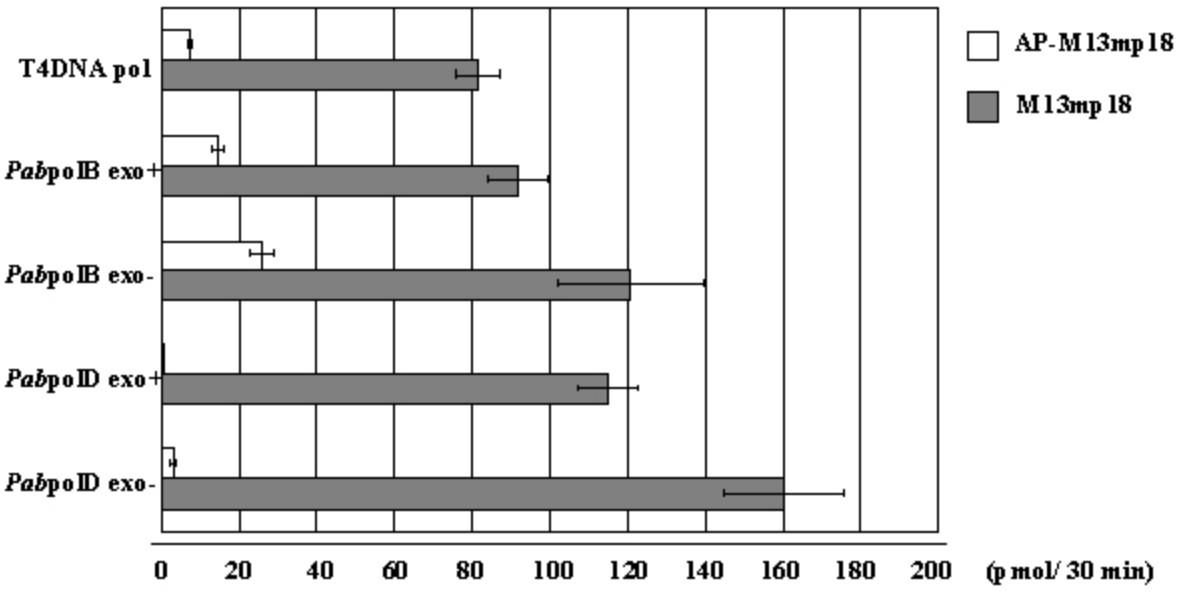
T4DNA pol
PabpoIB exo+
PabpoIB exo-
PabpoID exo+
PabpoID exo-
AP-M13mp18
M13mp18
0 20 40 60 80 100 120 140 160 180 200
(p mol/ 30 min)

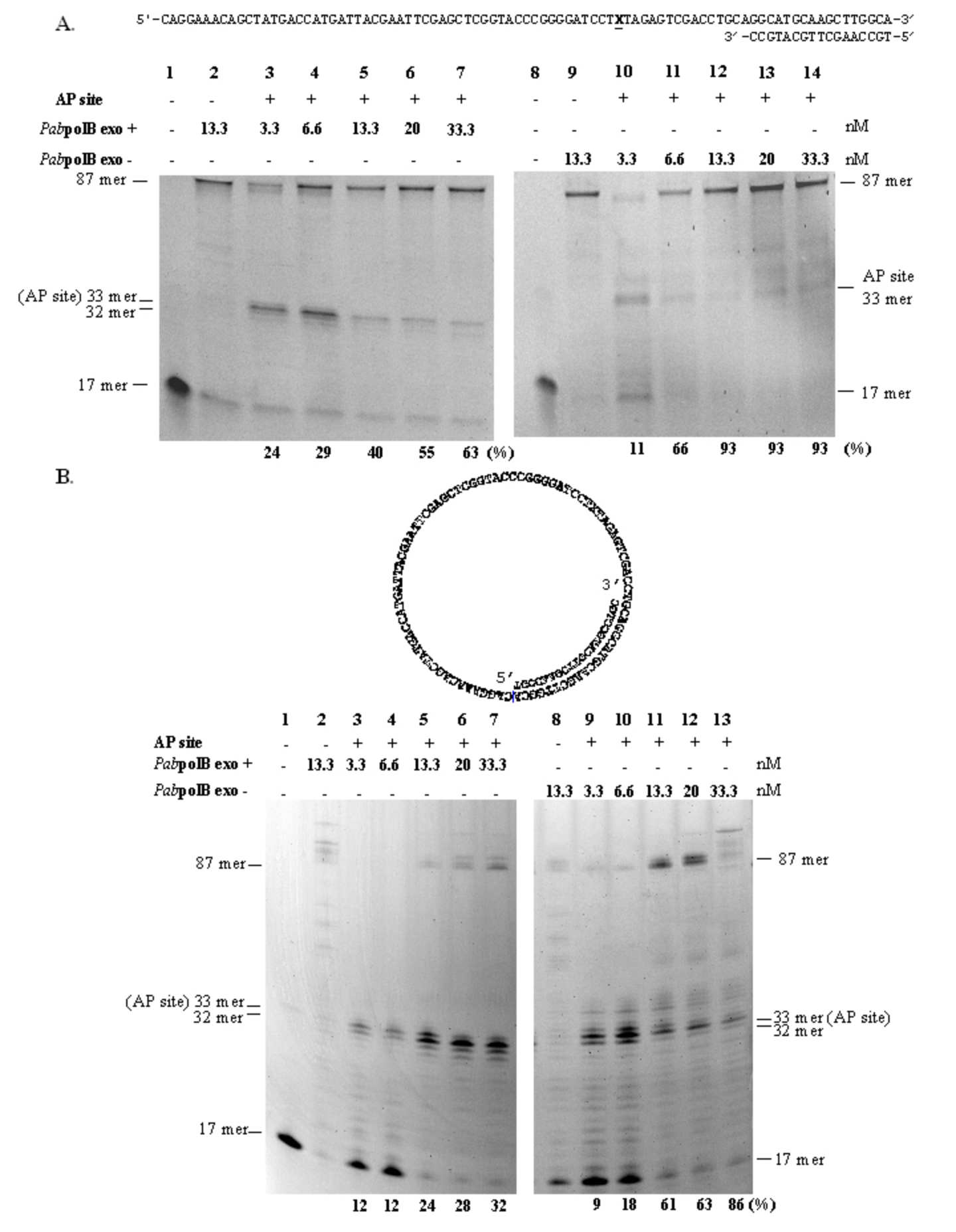
A.
5′-CAGGAAACAGCTATGACCATGATTACGAATTCGAGCTCGGTACCCGGGGATCCTXTAGAGTCGACCTGCAGGCATGCAAGCTTGGCA-3′
3′-CCGTACGTTCGAACCGT-5′
1 2 3 4 5 6 7 8 9 10 11 12 13 14
AP site - - + + + + + - - + + + + +
PabpolB exo + - 13.3 3.3 6.6 13.3 20 33.3 - - - - - - - nM
PabpolB exo - - - - - - - - - 13.3 3.3 6.6 13.3 20 33.3 nM
87 mer
(AP site) 33 mer
32 mer
17 mer
AP site
33 mer
24 29 40 55 63 (%)
11 66 93 93 93 (%)
B.
3′
5′
1 2 3 4 5 6 7 8 9 10 11 12 13
AP site - - + + + + + - + + + + + +
PabpolB exo + - 13.3 3.3 6.6 13.3 20 33.3 - - - - - - nM
PabpolB exo - - - - - - - - 13.3 3.3 6.6 13.3 20 33.3 nM
87 mer
(AP site) 33 mer
32 mer
17 mer
33 mer (AP site)
12 12 24 28 32
9 18 61 63 86 (%)

Figure 3

A.

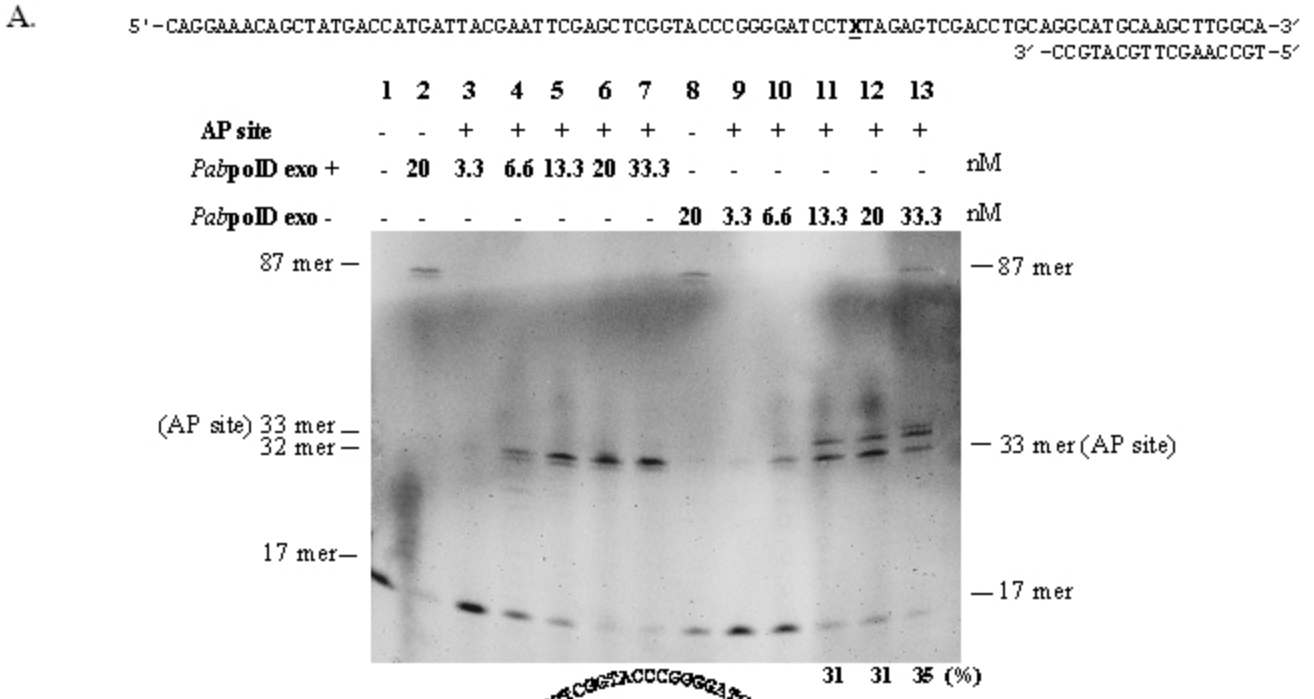

B.

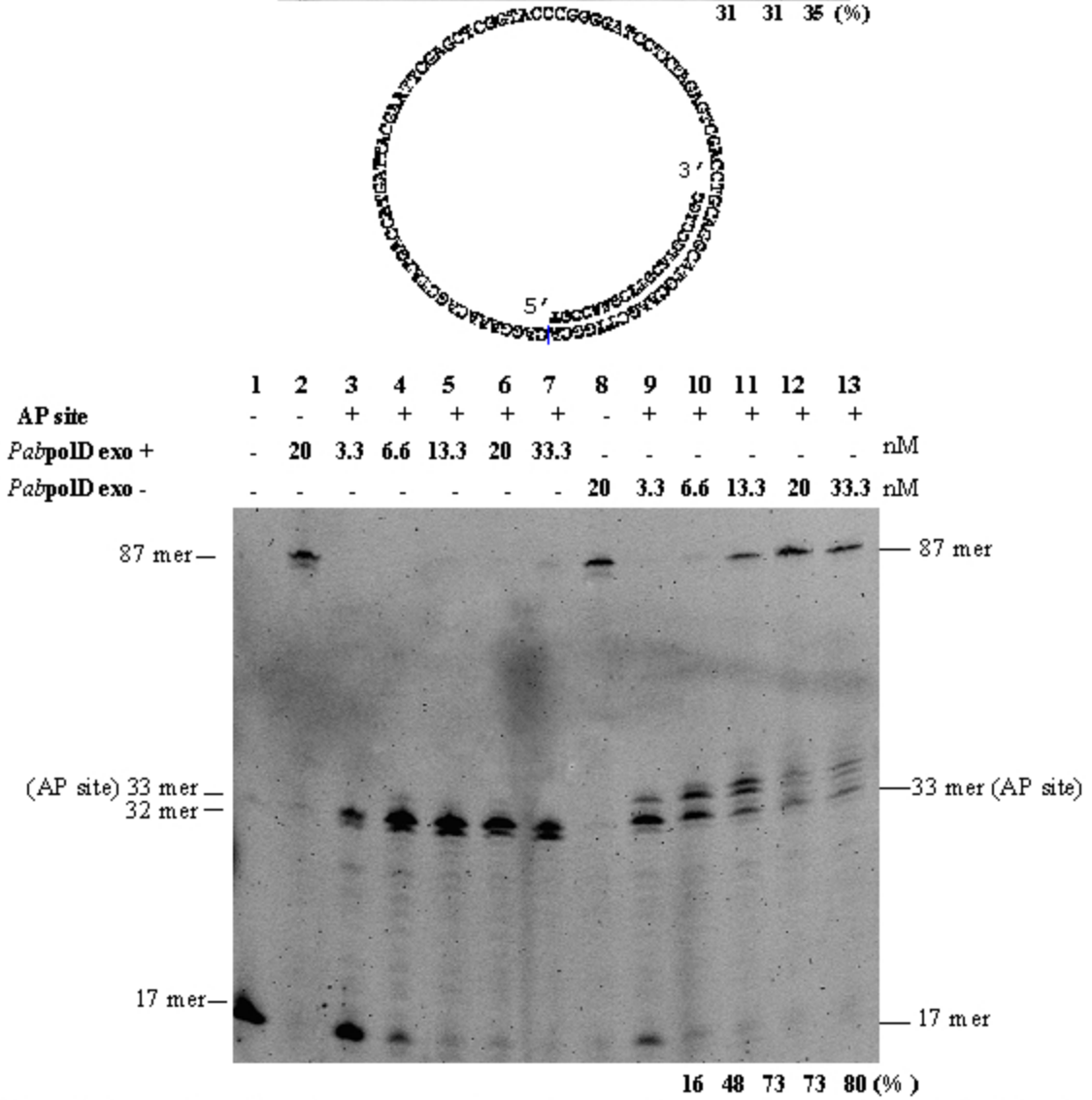

Figure 4 : Replication of AP-containing mini-circular and linear oligonucleotides DNA templates by the wild-type or exonuclease-deficient *Pab*polD

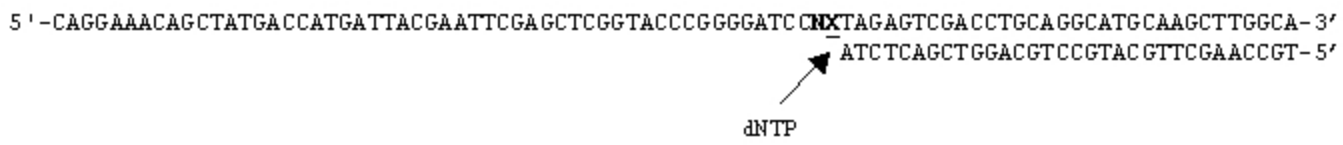

A.

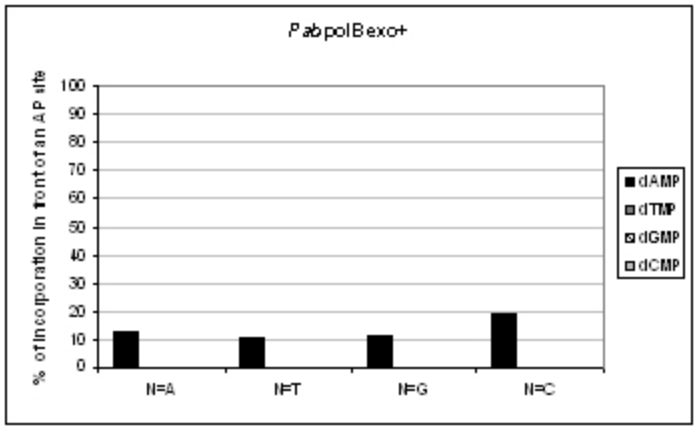

B.

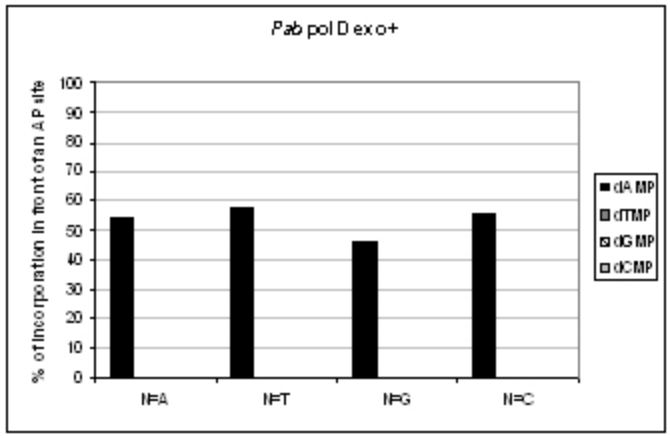

C.

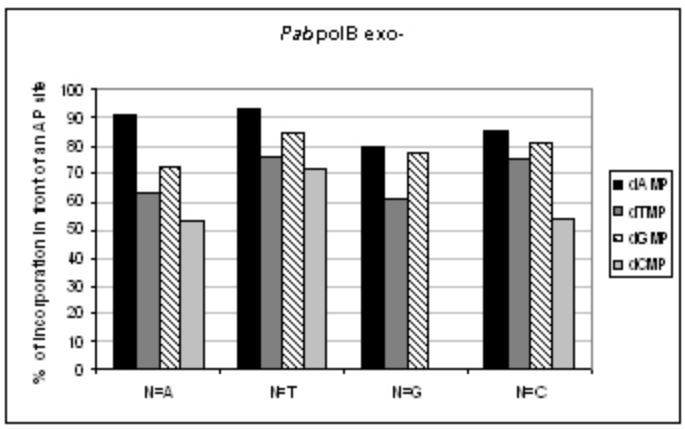

D.

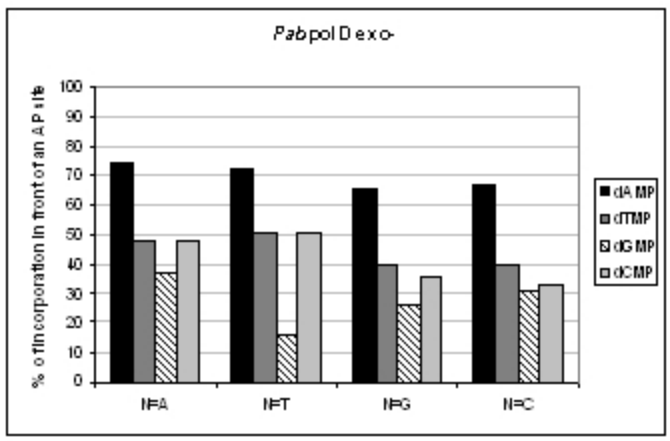

Figure 5

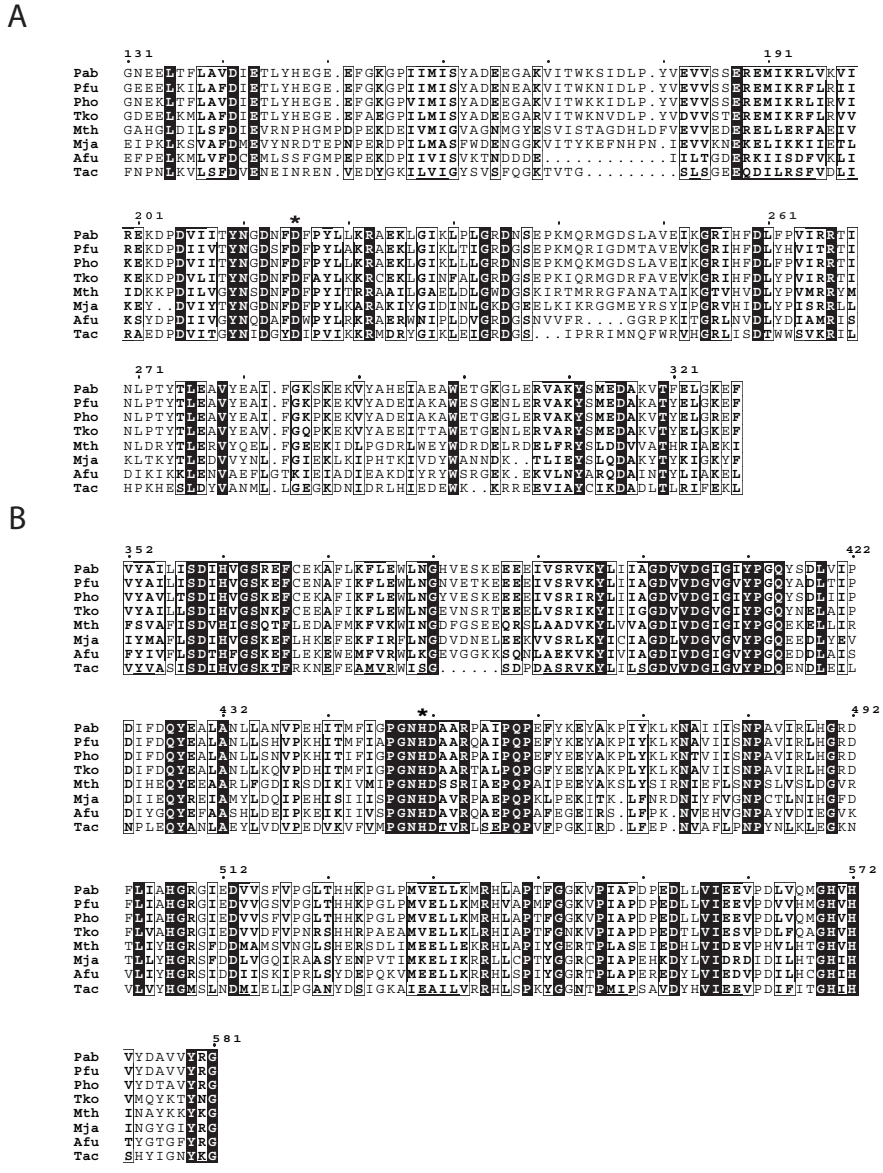

Figure S1: Mapping of conserved residues involved in 3'-5' exonuclease activity among representative euryarchaeal DNA polymerases.

A, Sequence alignment of the exonuclease domain in representative family B DNA polymerases. The sequences are from eight euryarchaeota species, *P. abyssi* (Pab, accession number, gi:14521919), *P. furiosus* (Pfu, accession number, gi:18976584), *P. horikoshii* (Pho, accession number, gi:14591688), *T. kodakarensis* KOD1 (Tko, accession number, gi:57639936), *M. thermoautotrophicum* (Mth, accession number, gi:15679219), *M. jannashii* (Mja, accession number, gi:15669075), *A. fulgidus* (Afu, accession number, gi:11498108), *T. acidophilum* (Tac, accession number, gi:16081956). The star indicates the identified residue in *Pab*polB responsible for proofreading activity. **B**, Partial sequence alignment of the small subunits (DP1s) of the family D DNA polymerases. The sequences are from eight euryarchaeota species, *P. abyssi* (Pab, accession number, gi:14520339), *P. furiosus* (Pfu, accession number, gi:18976390), *P. horikoshii* (Pho, accession number, gi:14590067), *T. kodakarensis* KOD1 (Tko, accession number, gi:57641837), *M. thermoautotrophicum* (Mth, accession number, gi:15679404), *M. jannashii* (Mja, accession number, gi:15668883), *A. fulgidus* (Afu, accession number, gi:11499379), *T. acidophilum* (Tac, accession number, gi:16081371). The star indicates the identified residue in *Pab*DP1 responsible for proofreading activity. Amino acid sequence alignments have been constructed by ClustalW2. Numbering refers to *P. abyssi* amino acid sequences.

A.

Figure S2

5'-CAGGAAACAGCTATGACCATGATTACGAATTCGAGCTCGGTACCCGGGGATCCT**C**TAGAGTCGACCTGCAGGCATGCAAGCTTGGCA-3′
ATCTCAGCTGGACGTCCGTACGTTCGAACCGT-5′

dNTP incorporation opposite undamaged nucleotide C

***Pab*polB exo +**

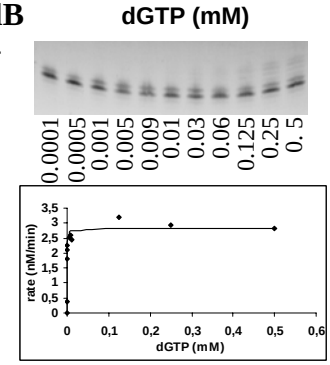

***Pab*polD exo +**

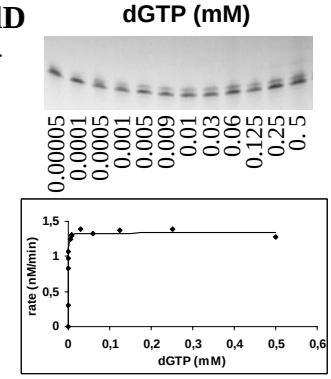

***Pab*polB exo -**

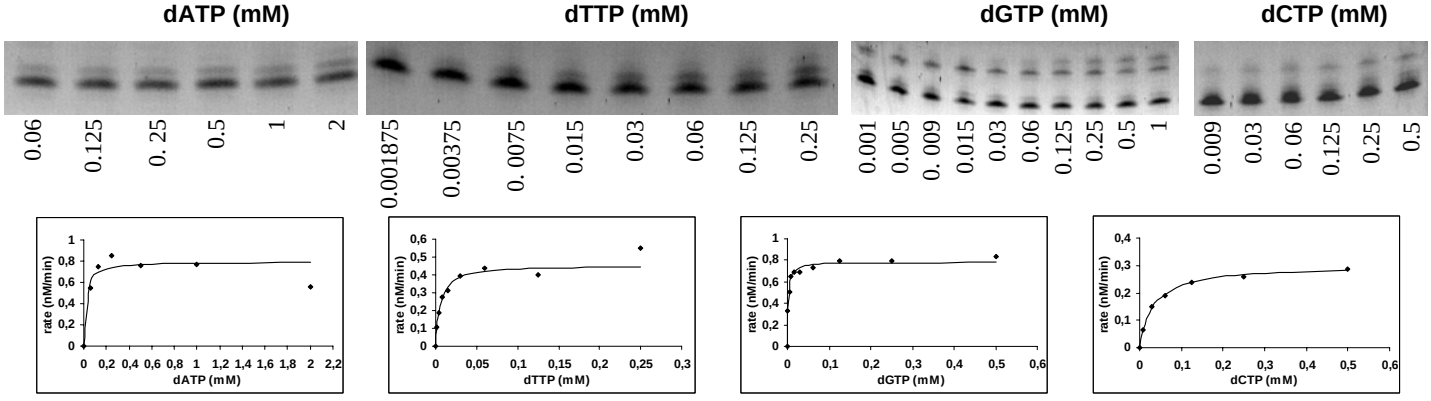

***Pab*polD exo -**

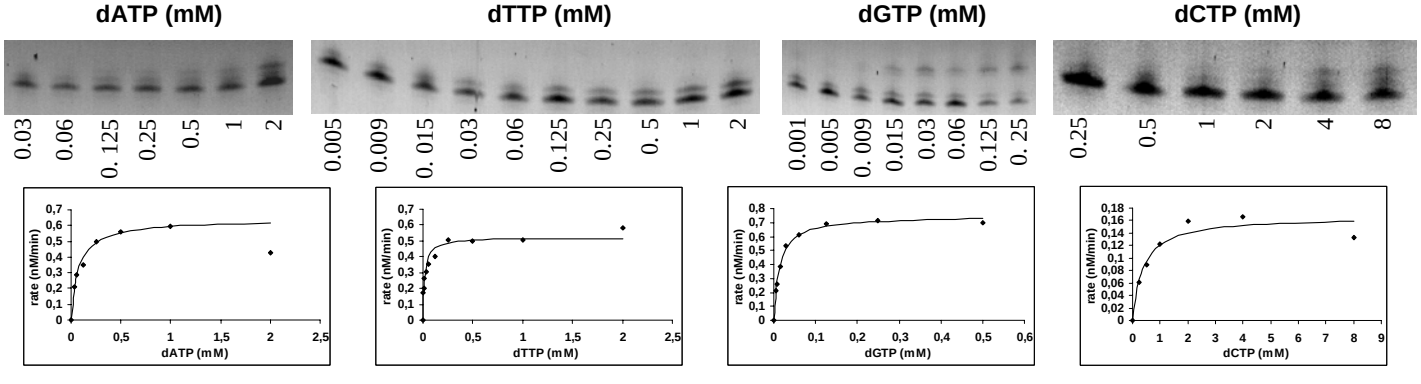

B.

5'-CAGGAAACAGCTATGACCATGATTACGAATTCGAGCTCGGTACCCGGGGATCCT**X**TAGAGTCGACCTGCAGGCATGCAAGCTTGGCA-3′

ATCTCAGCTGGACGTCCGTACGTTCGAACCGT-5′

dNTP incorporation opposite an AP site

***Pab*polB exo +**

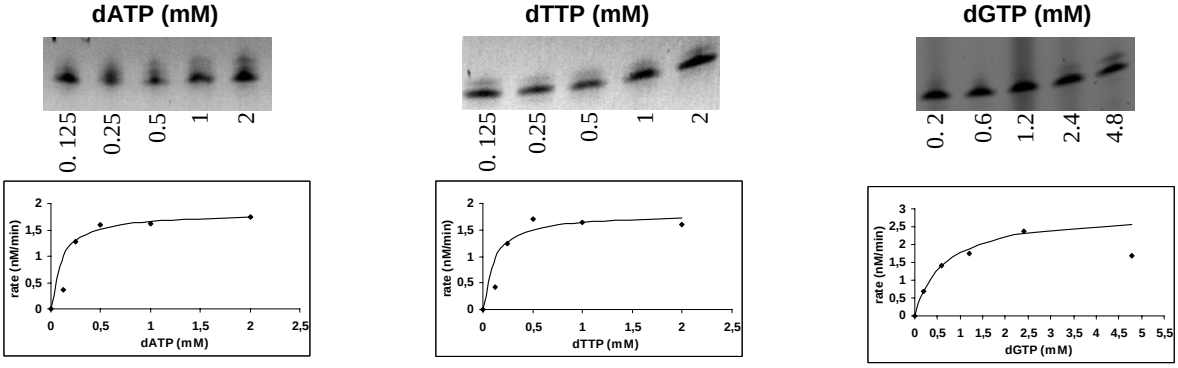

***Pab*polD exo +**

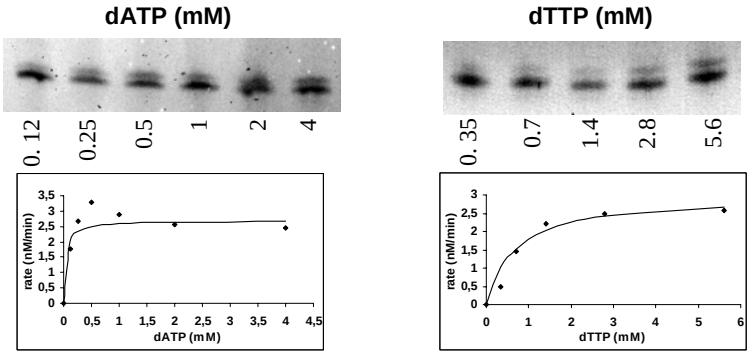

***Pab*polB exo -**

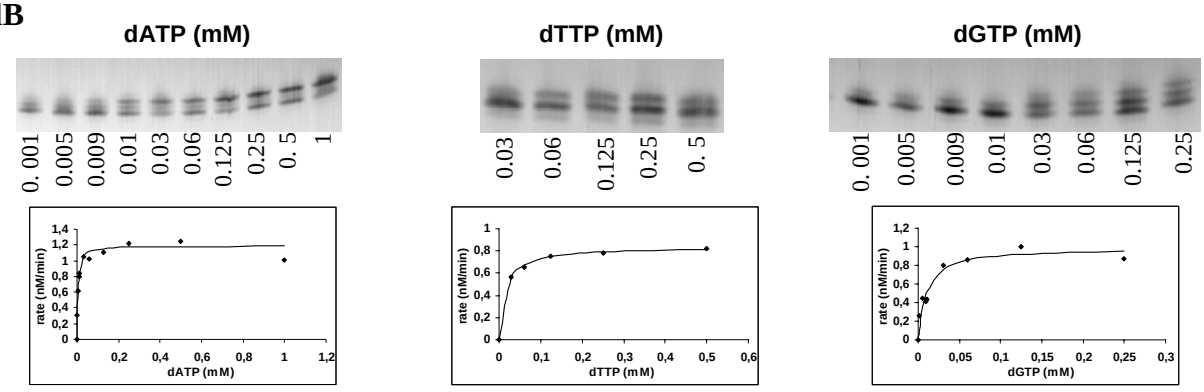

***Pab*polD exo -**

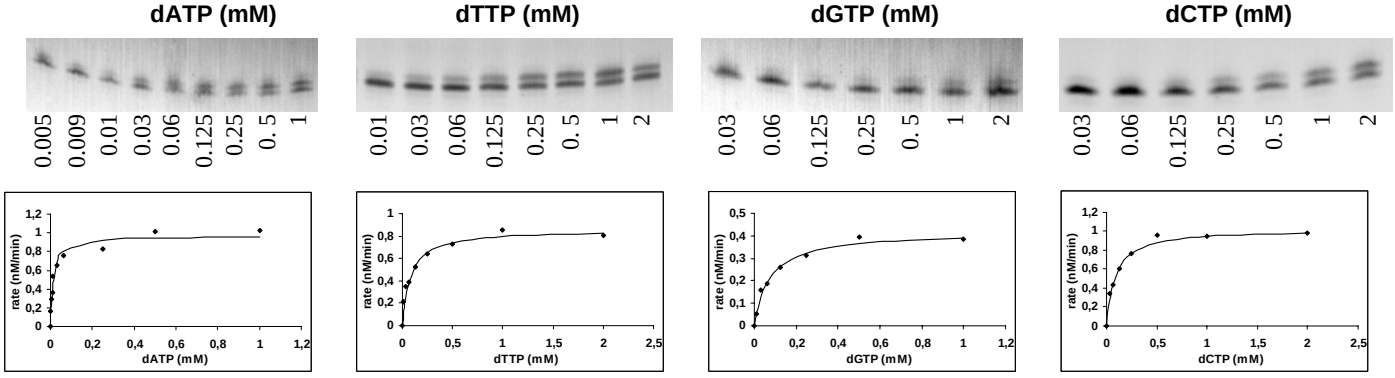

Figure S2: Steady-state kinetics analyses of deoxynucleotide incorporation by *Pab*pols.
A, Incorporation of dNTP opposite undamaged C. The primer-template duplex (8.3 nM) was incubated individually with *Pab*polB exo+ (6.6 nM), *Pab*polD exo+ (20 nM), *Pab*polB exo- (13 nM) or *Pab*polD exo- (16 nM), in the presence of a single dNTP at the indicated concentrations. **B**, Incorporation of dNTP opposite an AP site. The primer-template duplex (8.3 nM) was incubated individually with *Pab*polB exo+ (24 nM), *Pab*polD exo+ (20 nM), *Pab*polB exo- (13.3 nM) or *Pab*polD exo- (33.3 nM), in the presence of a single dNTP at the indicated concentrations. Reactions were carried out at 55°C under standard *Pab*pols assay conditions and the products were resolved by denaturing PAGE. The rate of incorporation was graphed as a function of dNTP concentration and the data were fit to the Michaelis-Menten equation. The k_{cat} et K_m parameters obtained from the fit are listed in Table 2.